WPEC Subgroup 34

"Coordinated evaluation of ^{239}Pu in the resonance region"

Monitor: R. D. McKnight (ANL, USA)
Coordinator: C. De Saint Jean (CEA, France)

1. Introduction

In recent history, the United States and Europe have adopted the same evaluation for the ^{239}Pu resonance region, largely based on work from the Oak Ridge National Laboratory (ORNL, USA) and the French Atomic Energy Commission (CEA Cadarache). In data testing for ENDF/B-VII.0, a general over prediction of Pu-SOL-THERMAL assemblies was noted, with an over prediction of typically about 0.5% - a very serious discrepancy indeed. Testing of the new evaluation in intermediate assemblies also shows a very large (and unwanted) increase in the C/E's.

In recent years, two efforts should be mentioned. Firstly, the JEFF community has developed an updated ^{239}Pu file for JEFF-3.1.1 with modifications to the original JEFF-3.1 file, at thermal energies, that has improved some of the aforementioned discrepancies. Secondly, at ORNL, Derrien and Leal have developed a new set of resonance parameters that have been incorporated into a file in ENDF/A for testing. This most recent evaluation is more consistent with the cross-section resonance data and believed by the evaluators to be the best representation of these data to date. Nonetheless, this new evaluation does not improve the poor integral performance of the ENDF/B-VII.0 file, and in fact most of the discrepancies become slightly worse, as was noted by McKnight at the June 2009 CSEWG meeting.

The goal of this subgroup is to bring together the OECD/NEA experts in this area to see if a new evaluation can be developed that both uses the most accurate fundamental cross-section data with nuclear theory constraints, and also better predicts the relevant integral criticality data.

2. Tasks

To obtain an improvement of ^{239}Pu resonances both on the microscopic and integral experiments point of view, several tasks were proposed at the beginning of this subgroup activity:

- Evaluation tasks:
  - ^{239}Pu resolved resonance range with covariances,
  - ^{239}Pu unresolved resonances range with covariances,
  - ^{239}Pu fission spectra (chi).
  - ^{239}Pu nu-bar in the thermal range as well as in the resonance range.
- Benchmarking tasks:
  - Define a set of public benchmarks related to ^{239}Pu nuclear data: ICSBEP and IRPhEP,
  - Calculations of these benchmarks with various evaluations (ENDF, JEFF, JENDL, ...),
  - Spot as far as possible (via perturbation analysis) possible nuclear data improvements.

In addition, the subgroup had in mind to take into account various activities that might be related to ^{239}Pu:

- Insure a proper link with Subgroup 32 on the unresolved treatment.
- "Background" information analysis:
  - We note that LANL has done simulations to test the impact of various prompt neutron spectra on criticality, and found a significant sensitivity of the results to the chi matrix adopted. The proposed WPEC subgroup should take advantage of ongoing work, coordinated by a new IAEA CRP, on the prompt fission neutron spectrum.
  - Fast region evaluations (JEFF, ENDF) and the corresponding partial cross-section splits: contributions from capture, inelastic, etc. are quite different and differences between various evaluations for inelastic scattering were pointed out.
- Initiate or target if needed new microscopic measurements.

The general strategy of this subgroup is synthesised in Figure 1.

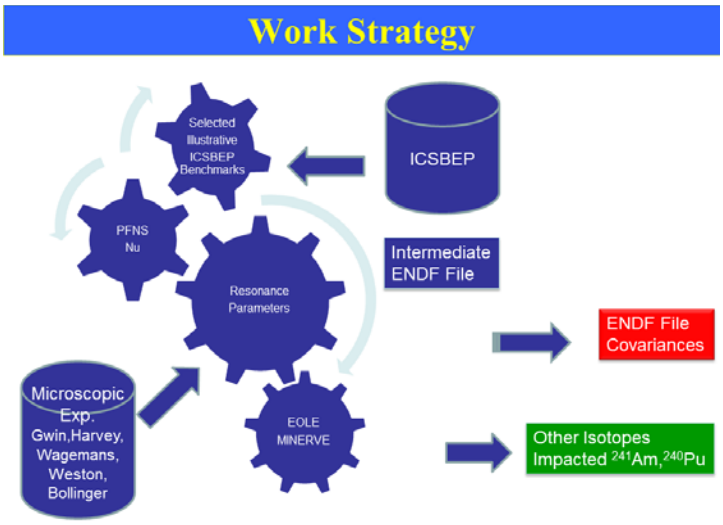

Figure 1: General strategy used in subgroup 34 for of ^{239}Pu resonances energy range.

3. Illustrative ICSBEP benchmark: description and initial results

3.1. Initial result with ENDF library

An over-prediction in calculated reactivity (k_{eff} for Pu fuelled systems, particularly thermal solution systems) has been a known issue for many years. This is illustrated in Figure 2 where we display the k_{eff} C/E results for a suite of over 150 International Criticality Safety Benchmark Evaluation Project (ICSBEP) Pu-SOL-THERM configurations [1].

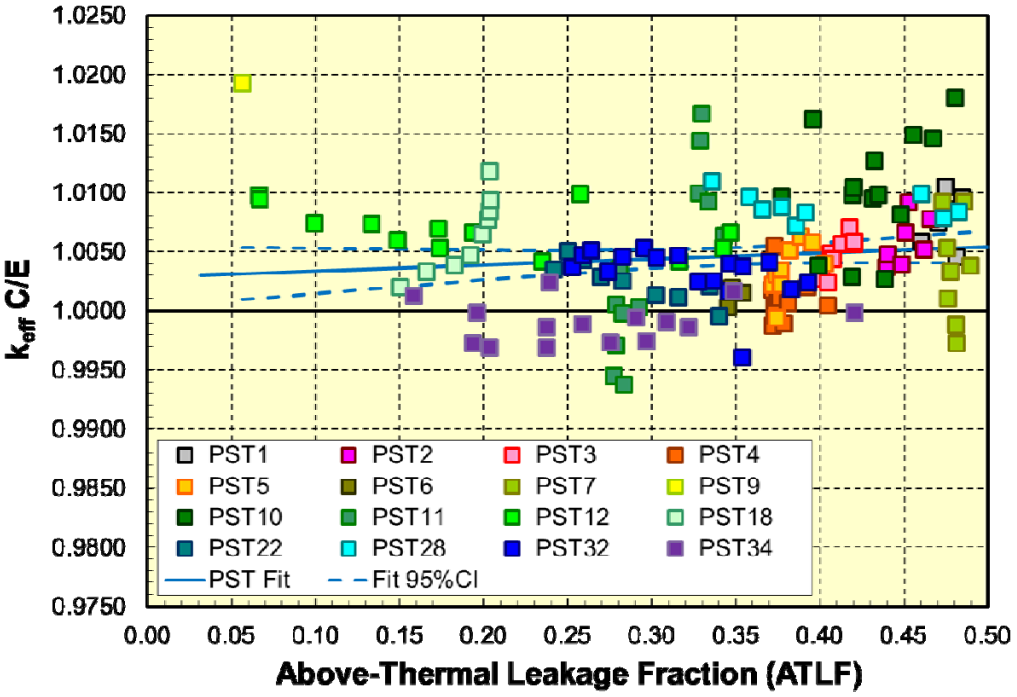

Figure 2: C/E results for Pu-SOL-THERM configurations based on ENDF/B-VII-1.

These results were obtained using LANL's MCNP6.1 [2] continuous energy Monte Carlo code and ENDF/B-VII.1 cross-sections (.80c ACE files and the associated .20t thermal kernels). Similar results have been obtained in the past with other cross-section files such as JEFF-3.1.1 and JENDL-4.0.

Included in Figure 2 is a linear fit versus the abscissa's "Above Thermal Leakage Fraction" (ATLF). This parameter has been used in the past when calculating thermal solution of Highly Enriched Uranium (HEU) systems. If the benchmark measurements and underlying nuclear data are accurate we would expect to obtain a regression equation whose intercept, or bias, term plus or minus its uncertainty brackets unity and whose slope, or trend, term plus or minus its uncertainty brackets zero. The latter goal is attained, as the trend term and its 95% confidence interval for this fit is $+0.0051 \pm 0.0073$ but there is evidence for a bias as the intercept term is 1.0029 ± 0.0026.

Similar fits can be made for k_{eff} C/E versus other parameters, including "Above Thermal Fission Fraction (ATFF)", ^{239}Pu/Pu atom fraction, grams Pu/liter of solution or Hydrogen-to-Pu in solution ratio. Regression analyses generally yield intercept terms indicative of a **500 pcm** or so bias.

3.2. Initial result with JEFF libraries (from JEFF-3.1 to JEFF-3.1.1)

It was noted in 2006 that for JEFF-3.1, ICSBEP/PU-SOL-THERM Benchmarks show an overestimation of the k_{eff} prediction [3,4]. Figure 3 presents some results insisting on this issue for a limited set: PST001 to PST011 (^{240}Pu content < 4.8%) and PST012 (^{240}Pu content =19%). This overestimation was pointed to be between 340 and 700 pcm.

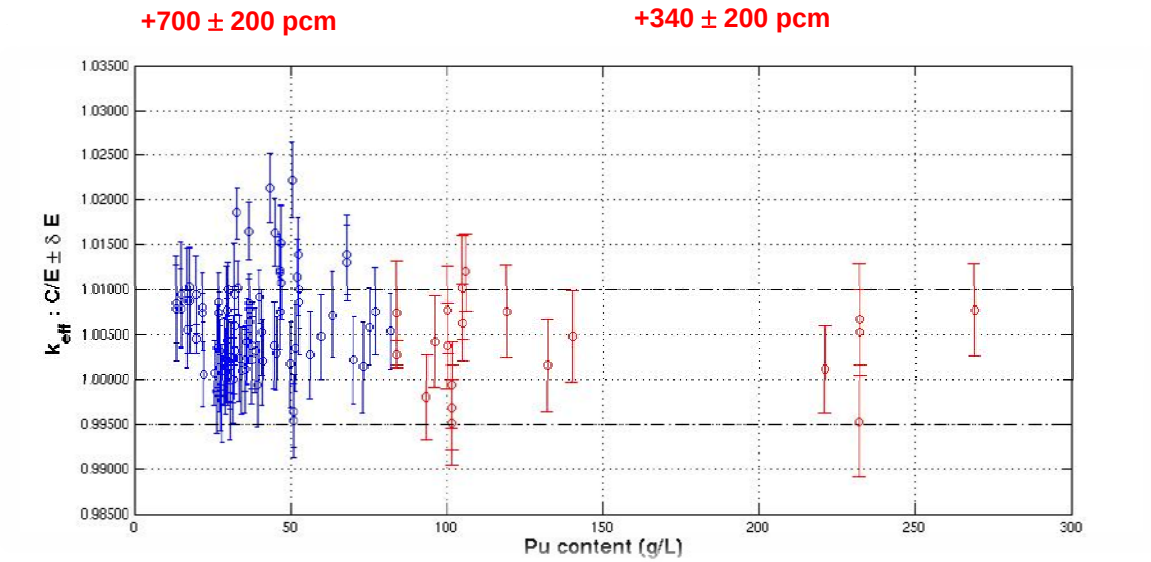

Figure 3: C/E results for Pu-SOL-THERM configurations based on JEFF-3.1 [3]

JEFF participants thus proposed a revised ^{239}Pu evaluation showing a better overall integral behaviour regarding the PST suite. This evaluation was part of JEFF-3.1.1 library. As mentioned in JEFF Report 22 [5] and by Reference [6], an overall remaining biased of around +250pcm was found at that time with this latter JEFF version for Pu-Sol-Therm with Pu concentration < 80 g/l and around +50 pcm for Pu-Sol-Therm with Pu concentration >80 g/l. Additional benchmarks were evaluated on various 100% MOX experiments performed in EOLE since 1993, using the same MOX 7%Pu fuel pins. These successive MH1.2, MISTRAL2 and MISTRAL3 experiments were carried out respectively in 1993, 1997 and 1999. A remaining bias was spotted mainly due to ^{241}Am.

3.3. Selected ICSBEP Pu-SOL-THERM set

As a new ^{239}Pu evaluated nuclear data files will be available it is neither necessary nor practical to re-calculate the reactivity for all critical configurations. Rather we have selected a small subset of these benchmarks whose attributes span the phase space defined by these parameters. The selected benchmarks are defined in Table 1.

Table 1: PST Benchmarks and Associated Parameters

Benchmark Name	Benchmark Parameter
PST12.13 – PST1.4	Above-Thermal Leakage Fraction (ATLF)
PST12.10 – PST34.14	Above-Thermal Fission Fraction (ATFF)
PST18.6 – PST4.1	^{239}Pu/Pu Atom Percent (a/o)
PST12.10 – PST34.3	Grams Pu / Liter of Solution (g Pu/l)
PST34.14 – PST9	Hydrogen to Pu (H/Pu) in Solution

The average k_{eff} C/E for all PST benchmarks, calculated with ENDF/B-VII.1 cross-sections is 1.0046 while the average k_{eff} C/E for the 8 sample subset is 1.0058, supporting the assertion that this subset of benchmarks adequately represents the complete population.

4. Re-evaluation of the ^{239}Pu Resolved Resonance Parameters in the Energy Range 10^{-5} eV to 2.5 keV

4.1. Introduction

A collaborative effort between the Oak Ridge National Laboratory (ORNL) and The French Atomic Energy Commission (CEA/Cadarache) was initiated under the auspice of the US Department of Energy and the Nuclear Energy Agency (NEA) to address issues pertinent to the performance of the ^{239}Pu cross-sections in benchmark calculations. Researcher L. Leal from ORNL travelled to Cadarache to work with G. Noguere for two months on the analysis and evaluation of the ^{239}Pu in the resolved resonance region. The following tasks were performed:

1. Use the SAMMY [7] code to perform resonance analysis using the best selected set of experimental time-of-flight data;
2. Generate cross-section library with the NJOY [8] code for use in benchmark calculations with the MCNP [2] code;
3. Generate cross-section library with the GALILEE (NJOY+CALENDF) code [9] for use in benchmark calculations with the TRIPOLI [10] and APOLLO [11] codes;
4. Use a selected set of experimental benchmarks with average of neutron lethargy causing fission spanning the energy range from 0.01 eV to 3 eV;
5. Use MISTRAL and FUBILA experiments (MOX fuel) performed at the EOLE facility to test the evaluation;
6. Evaluate nu-bar to improve benchmark results;

4.2. General Descriptions

In the eighties and early nineties H. Derrien and others [12,13] performed a ^{239}Pu evaluation in a collaborative work including CEA and ORNL. At that time, due to computer limitations for data storage and processing decision was made to split the resonance region in three parts, namely, 10^{-5} eV to 1 keV, 1 keV to 2 keV, and 2 keV to 2.5 keV. The evaluation was accepted for inclusion in the ENDF and JEFF nuclear data libraries. The evaluation is included in the latest release of ENDF, the ENDF/B-VII.1 and is also in the JEFF-3.1 libraries. While the evaluation was performed based on high-resolution data, mainly transmission data [14] taken at the Oak Ridge Electron Linear Accelerator (ORELA) at ORNL, no benchmark testing was done at the time the evaluation was released. Later on benchmark calculations indicated deficiencies on the ^{239}Pu evaluation in reproducing integral results. Also some additional issues with the evaluation arise from the use of three distinct sets of resonance parameters. The cross-sections calculated at the energy boundary of two consecutive disjoint resonance parameter sets could be different leading to discontinuity. Another concern relates to data uncertainty assessment using resonance parameter covariance. For data uncertainty analysis the use of a single resonance parameter set covering the entire energy region would be preferable since the disjoint set of resonance parameters do not permit the

determination of a fully uncertainty correlation in the entire energy region. Hence, decision was made to combine the three sets of resonance parameters and re-do the evaluation. The task was achieved since computer resources had substantially improved. As a result, a resonance parameter evaluation was carried out by Derrien [15] covering the energy range 10^{-5} eV to 2.5 keV. Nevertheless the evaluation was unable to improve benchmark results. The evaluation was not proposed for inclusion in either ENDF or JEFF project.

To improve benchmark results an effort was taken by D. Bernard and others [16] at CEA/Cadarache to re-evaluate the ^{239}Pu resonance parameters and nu-bar. Since the resonance evaluation for the whole energy region was not available at the time, the work performed by Bernard was based on the JEFF-3.1 evaluation, i.e., with the three disjoint sets of resonance parameters. Bernard's evaluation considerably improved the results of benchmark calculations.

4.3. ORNL/CEA New ^{239}Pu Evaluation in the energy range 10^{-5} eV to 2.5 keV

4.3.1. Resonance Parameter Evaluation Procedure

With the set of resonance parameters covering the energy region up to 2.5 keV a good set of external resonance parameters were determined. The technique used for deriving the external levels is that described in Reference [17]. Six resonance levels with negative energies and nine levels above 2.5 keV were enough to represent the external resonances interference effect in the energy region 10^{-5} eV to 2.5 keV. The first negative level (close to zero) has a neutron width very small. It does not contribute much to the interference effect in the resonance region. However, it is used to get a representation in the shape of eta (η) that bends down at very low energy [18]. Figure 4 shows the cross-section shape in the resonance region due only to the external energy resonance levels. It should be noted that the cross-section value converges to 11.13 barns, which represents the potential cross-section for ^{239}Pu determined with an effective scattering radius of 9.41 fm. This feature indicates that the external levels contribution to the cross-section in the energy range10^{-5} eV to 2.5 keV is appropriate.

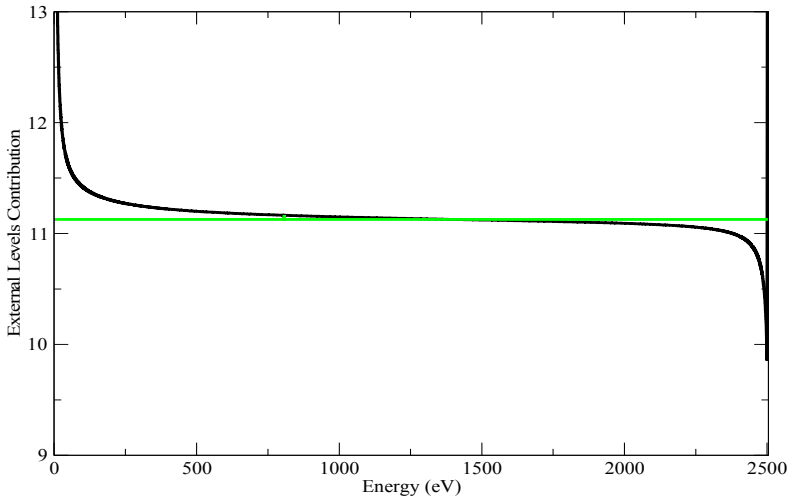

Figure 4: Contribution of the external levels in the resonance region.

The experimental database used in the new evaluation is essentially the same as that used by Derrien [15]. However, information derived from the knowledge of benchmark calculation results was also included in the SAMMY analysis together with the fitting of the differential data. Two quantities were essential in determining the best set of resonance parameters that fitted the experimental differential data and improving the benchmark results. The two quantities are η and the effective K1. These quantities are defined as:

$$\eta = \frac{\nu\sigma_f}{\sigma_a} = \frac{\nu}{1+\alpha} \quad , \tag{1}$$

where

$$\alpha = \frac{\sigma_\gamma}{\sigma_f} \quad ,$$

and

$$K1 = \bar{\nu}\sigma_{0f} g_f - \sigma_{0a} g_a \quad . \tag{2}$$

The cross-sections σ_{0f} and σ_{0a} are, respectively, the fission and absorption cross-sections at the thermal energy (0.0253 eV), whereas g_f and g_a are the Westcott's g-factors. The $\bar{\nu}$ value used in calculating the effective K1 from Equation (2) is taken at thermal energy. It was noted that the benchmark results were very sensitive to these two parameters. The benchmark results indicated that in some cases the sensitivity to K1 was more significant than on η. The K1 value for ^{239}Pu is higher than that of other major isotopes. For instance, for ^{235}U K1 value is around 722 barns whereas for ^{239}Pu it is 1160 barns.

An example of the SAMMY fit of the experimental differential data is displayed in Figure 5 for the total cross-section of Bollinger [19], fission cross-section of

Wagemans [20], and capture cross-section of Gwin [20] in the energy region from 0.01 eV to 3 eV.

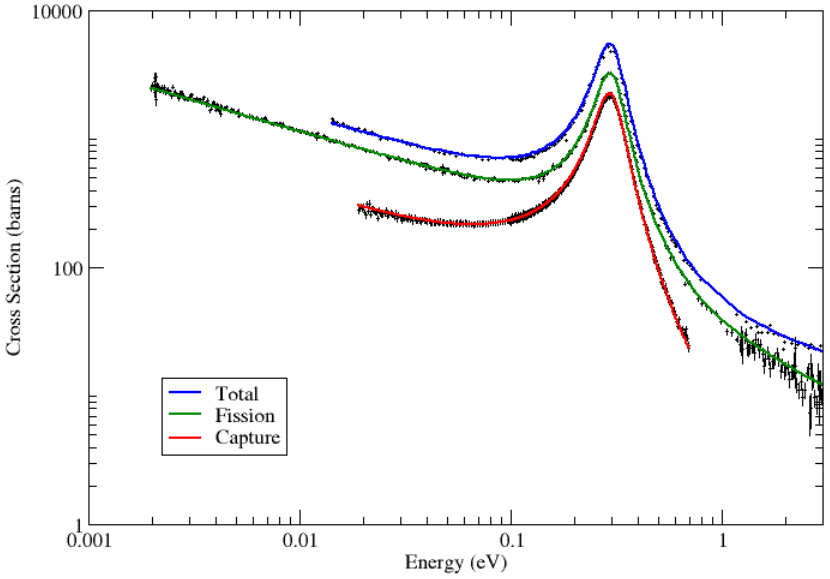

Figure 5: Results of SAMMY fit of the total, fission and capture cross-section data.

Values of the cross-section at thermal (0.0253 eV), fission Westcott factors, thermal $\bar{\nu}$, resonance integrals and K1 value are shown in Table 2. The unit for cross-sections, K1 and resonance integral is barns whereas the Westcott factor is dimensionless. Also, shown in Table 2 are the values listed in the Atlas of Neutron Resonance (ANR) [22], ENDF/B-VII.1 (same as JEFF-3.1), and the values calculated using Bernard's evaluation that is included in JEFF-3.1.1. The thermal cross-section values listed in the ANR were used in the SAMMY evaluation. The values listed in Table 2 were calculated with the SAMMY code.

Table 2: Thermal values and integral quantities calculated with SAMMY.

Quantity	ANR	ENDF/B-VII.1 (JEFF-3.1)	JEFF-3.1.1	ORNL/CEA
σ_γ	269.3 ± 2.9	270.64	272.72	270.06
σ_f	748.1 ± 2.0	747.65	747.08	747.19
g_f	1.0553 ± 0.0013	1.0544	1.0495	1.0516
g_a	1.0770 ± 0.0030	1.0784	1.0750	1.0771
$\bar{\nu}$	2.879 ± 0.006	2.873	2.868	2.868
I_γ	180 ± 20	181.44	181.50	180.09
I_f	303 ± 10	302.60	303.58	309.09
$K1$	1177.25	1166.62	1156.35	1161.30

4.3.2. Benchmark Calculations

To verify the performance of the ^{239}Pu evaluation in benchmark calculations seven critical experiments were chosen from the International Criticality Safety Benchmark Evaluation Project (ICSBEP) in the International Handbook of Evaluated Criticality Safety Benchmark Experiments. These benchmark experiments consist of light water reflected spheres of plutonium nitrate solutions. The benchmarks, listed in Table 3, have the average of neutron lethargy causing fission (EALF) spanning the energy range of 0.01 eV to 3 eV. It should be noted that the uncertainty in these benchmarks are around 500 pcm.

Several resonance parameters were derived from the SAMMY fitting of the experimental differential data. Each time a resonance parameter was obtained with a satisfactory fitting of the differential data (a good chi-square) the SAMMY resonance parameter was converted in the ENDF format and inserted into the JEFF-3.1.1 by replacing the existing resonance parameter. The cross-section library created was then processed for use in Monte Carlo calculation using the MCNP code. The MCNP libraries were generated with the NJOY/ACER code. All the cross-section data for the remaining isotopes present in the benchmark experiments were taken from the ENDF/B-VII.0. The process from the SAMMY fitting of the experimental data to the MCNP calculation was automated, validated and tested.

Table 3: ICSBEP benchmarks used in the ^{239}Pu evaluation

Benchmark	Experimental k_{eff}	EALF (eV)
PU-SOL-THERM-001 case 4	1.0000 ± 0.0050	0.0154
PU-SOL-THERM-004 case 1	1.0000 ± 0.0047	0.0531
PU-SOL-THERM-012 case 10	1.0000 ± 0.0047	0.0535
PU-SOL-THERM-012 case 13	1.0000 ± 0.0047	0.0428
PU-SOL-THERM-018 case 6	1.0000 ± 0.0047	0.0761
PU-SOL-THERM-034 case 4	1.0000 ± 0.0047	0.231
PU-SOL-THERM-034 case 15	1.0000 ± 0.0047	2.730

Various k_{eff} results were obtained for the seven benchmark listed in Table 3. The impact of the cross-section change in the k_{eff} values were analyzed and it was noted that a very minor change in the thermal cross-section and in the first resonance around 0.2956 eV would change the k_{eff} value of the thermal benchmark listed in Table 3 significantly. In addition, results of sensitivity calculations using the TSUNAMI sequence of the SCALE code [23] indicated that to achieve a reasonable k_{eff} result a combined change on the nu-bar, on the fission and capture cross-sections values were needed as opposed to a simple change in one of these quantities alone. The very first attempt made was to focus on η (or α) since it involves these three quantities as indicated in Equation (1). However, further investigations indicated that the k_{eff} was also very sensitive to K1. Although no

experimental measurement of K1 was found in the literature for ^{239}Pu integral experiments performed at the MINERVE could be used to infer the value of K1 that provided the best results for reactivity changes. A values of K1 around 1161 barns indicated that a reasonable k_{eff} could be achieved for the seven benchmark listed in Table 3. Hence, in addition to fitting the experimental differential data SAMMY also fitted K1.

The benchmark results for the seven benchmark displayed in Table 3 are shown in Figure 6.

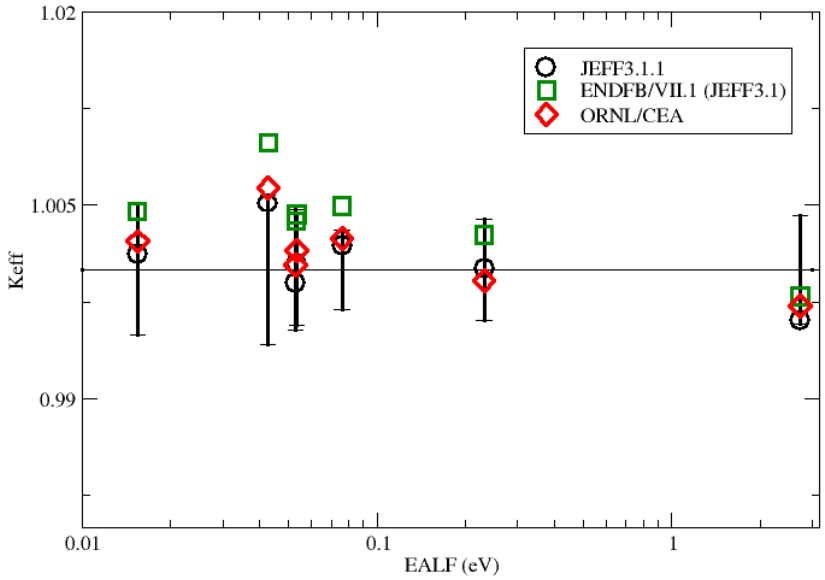

Figure 6: MCNP results for seven ICSBEP benchmarks listed in Table 3.

4.4. Resonance Parameter Covariance Matrix (RPCM)

The Resonance Parameter Covariance Matrix related to the parameters established in the frame of this subgroup was generated with the marginalization procedure of the CONRAD code [24]. The Governing equations and the results are given below.

4.4.1. Governing equations

The marginalization procedure of the CONRAD code is a mathematical technique designed to take into account experimental uncertainties of systematic origins in the uncertainty propagation calculations.

The neutron cross-section evaluation stands for a phenomenological description of a physical reality with a large number of parameters. Thousands of model parameters and experimental data points are needed to describe the main neutron reactions of interest for the nuclear applications. In practice, all of the model parameter covariances cannot be simultaneously estimated from well-defined sets of experimental data. The situation

becomes more and more complex when the number of open reaction channels increases. This optimization problem is non-convex in general, making it difficult to find the global optima.

A solution to simplify the problem consists of dividing the model parameter sequence into blocks of variables whose uncertainties can be propagated through fixed-order sequential data assimilation procedures. According to definitions and nomenclature used in statistics, we can identify the "observable," "latent," and "nuisance" variables. Observable variables can be directly determined from the experimental data. Latent variables as opposed to observable variables may define redundant parameters or hidden variables that cannot be observed directly. This term reflects the fact that such variables are really there, but they cannot be observed or measured for practical reasons. Nuisance variables, i.e. experimental corrections, correspond to the aspect of physical realities whose properties are not of particular interest as such but are fundamental for assessing reliable model parameters. As shown in References [25-27], marginalization techniques may provide appropriate solutions to propagate the nuisance and latent model parameters.

Here, only the uncertainty propagation of the observed and nuisance parameters is discussed. Therefore, the model parameters and the corresponding covariance matrix can be partitioned as:

$$\mu = \begin{pmatrix} x \\ \theta \end{pmatrix}, \qquad \Sigma = \begin{pmatrix} \Sigma_{11} & \Sigma_{12} \\ \Sigma_{21} & \Sigma_{22} \end{pmatrix},$$

In which $x=(x_1 \ \dots \ x_n)^T$ and $\theta=(\theta_1 \ \dots \ \theta_m)^T$ represent the observable parameter and nuisance parameters, respectively. In the resonance range of the neutron cross-sections, x_i are the resonance parameters and Σ_{11} stands for the Resonance Parameter Covariance Matrix (RPCM). The matrix Σ_{22} contains the variances and covariances of the nuisance parameters. The marginalization procedure can be mathematically expressed as follow:

$$\Sigma_{11} = M_x + H_\theta ,$$

where

$$H_\theta = \left(G_x^T G_x\right)^{-1} G_x^T G_\theta \Sigma_{22} G_\theta^T G_x \left(G_x^T G_x\right)^{-1} .$$

The matrix M_x is the posterior covariance matrix obtained at the end of the fitting procedure. The derivative matrices G_x and G_θ of the quantity z (reaction yield, transmission or neutron cross-section) to the parameter x and θ are defined as:

$$G_x = \begin{pmatrix} \frac{\partial z_1}{\partial x_1} & \cdots & \frac{\partial z_1}{\partial x_n} \\ \vdots & \ddots & \vdots \\ \frac{\partial z_k}{\partial x_1} & \cdots & \frac{\partial z_k}{\partial x_n} \end{pmatrix},$$

and

$$G_\theta = \begin{pmatrix} \frac{\partial z_1}{\partial \theta_1} & \cdots & \frac{\partial z_1}{\partial \theta_n} \\ \vdots & \ddots & \vdots \\ \frac{\partial z_k}{\partial \theta_1} & \cdots & \frac{\partial z_k}{\partial \theta_n} \end{pmatrix}.$$

A two-step CONRAD calculation is needed to obtain the covariance matrices M_x and H_θ. The first step consists of using the fitting procedure of CONRAD in order to determine M_x from well-defined sets of experimental data z of general dimension k. The second step consists of determining elements of H_θ by calculating the derivative matrices G_x and G_θ.

4.4.2. CONRAD results

For practical applications, the marginalization procedure was applied in the frame of a retroactive analysis. The latter analysis consists of calculating the covariances between the resonance parameters without changing their values. This can be achieved by replacing the experimental data with theoretical cross-sections. In this work, the retroactive analysis was applied on the fission and capture cross-sections.

The number of s-wave resonances established in this work is 1043. In order to overcome problems related to storage and processing of large RPCM, a neutron width selection was applied to reduce the size of the resonance parameter set. The selection principle relies on properties of the cumulative Porter-Thomas integral distribution. Figure 7 represents the histogram of the reduced neutron width divided by its mean value. The abscise x_0 is defined as:

$$x_0 = \frac{g\Gamma_n^0}{\left\langle g\Gamma_n^0 \right\rangle},$$

where g is the statistical spin factor. The smooth curve is given by:

$$N(x_0) = Nerfc\left(\sqrt{\frac{x_0}{2}}\right).$$

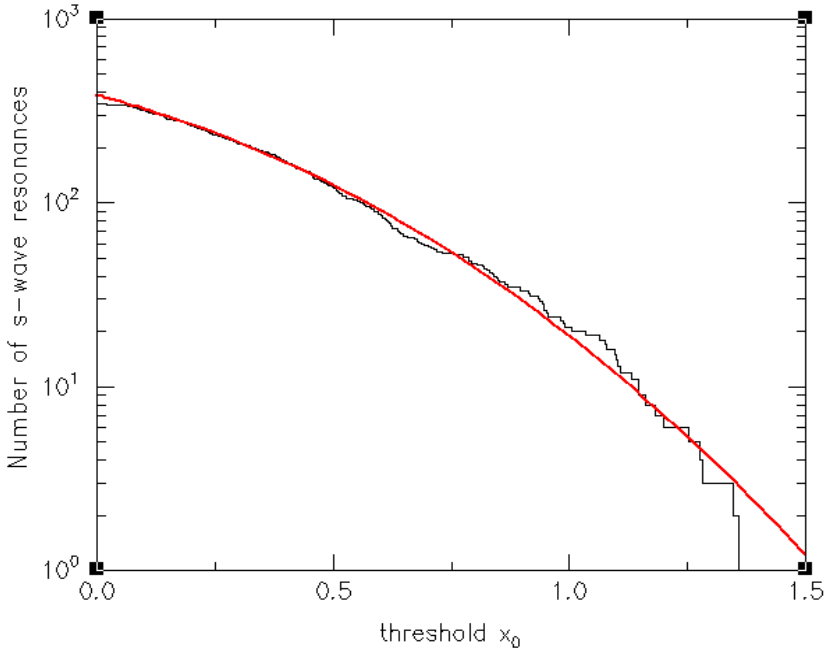

Figure 7: Cumulative Porter-Thomas integral distribution calculated with the neutron widths of the s-wave resonances observed below 1 keV.

At x_0=0, the number of s-save resonances is equal to:

$$N = \frac{E_{\max} - E_{\min}}{D_0} + 1,$$

Where E_{min} and E_{max} define the lower and upper energy limit of the energy range of interest and D_0 is the s-wave mean level spacing. For ^{239}Pu, the energy limits are E_{min}=0.3 eV and E_{max}=2.5 keV.

An s-wave resonance is included in the marginalization procedure if its reduced neutron width amplitude is larger than a threshold x_0. The latter threshold should fulfil the conditions $\sigma_{\gamma,g}(x_0=0)\approx\sigma_{\gamma,g}(x_0>0)$ for the capture cross-section and $\sigma_{f,g}(x_0=0)\approx\sigma_{f,g}(x_0>0)$ for the fission cross-section in a given energy group g. In this work, a broad energy mesh was used. This arbitrary choice allows removing three quarters of the s-wave resonances from the retroactive analysis. The final number of resonances is 302.

The energy domain was divided in three energy ranges to cover the thermal range, the first resonance at 0.3 eV and the resonance integral above 0.5 eV up to 2.5 keV. The final RPCM generated by CONRAD was converted in ENDF-6 format (MF=32, MT=151) and processed with the NJOY code. Results are shown in Figures 8 to 14. Table 4 reports the relative uncertainties for the total, fission, capture and elastic cross-sections.

Table 4: Relative uncertainties calculated for the total, capture, fission and elastic cross-sections.

Energy Range (eV)	Total cross-section	Capture cross-section	fission cross-section	elastic cross-section
E < 0.1	1.4 %	4.2 %	0.9 %	4.6 %
0.1 – 0.54	1.9 %	4.2 %	1.9 %	3.7 %
0.54 – 4.0	1.3 %	3.6 %	1.1 %	4.2 %
4.0 – 22.6	3.1 %	7.1 %	3.0 %	3.3 %
22.6 – 454.0	3.9 %	6.5 %	3.5 %	5.7 %
454.0 – 2500.0	3.2 %	5.1 %	3.2 %	4.0 %

In the RRR, the relative uncertainties for the fission and capture cross-sections remain below 3% and 7% respectively. The systematic uncertainties are the dominant components of the final uncertainties. As a consequence, simple correlation structures are obtained. The present results were included in the latest NEA library JEFF-3.2.

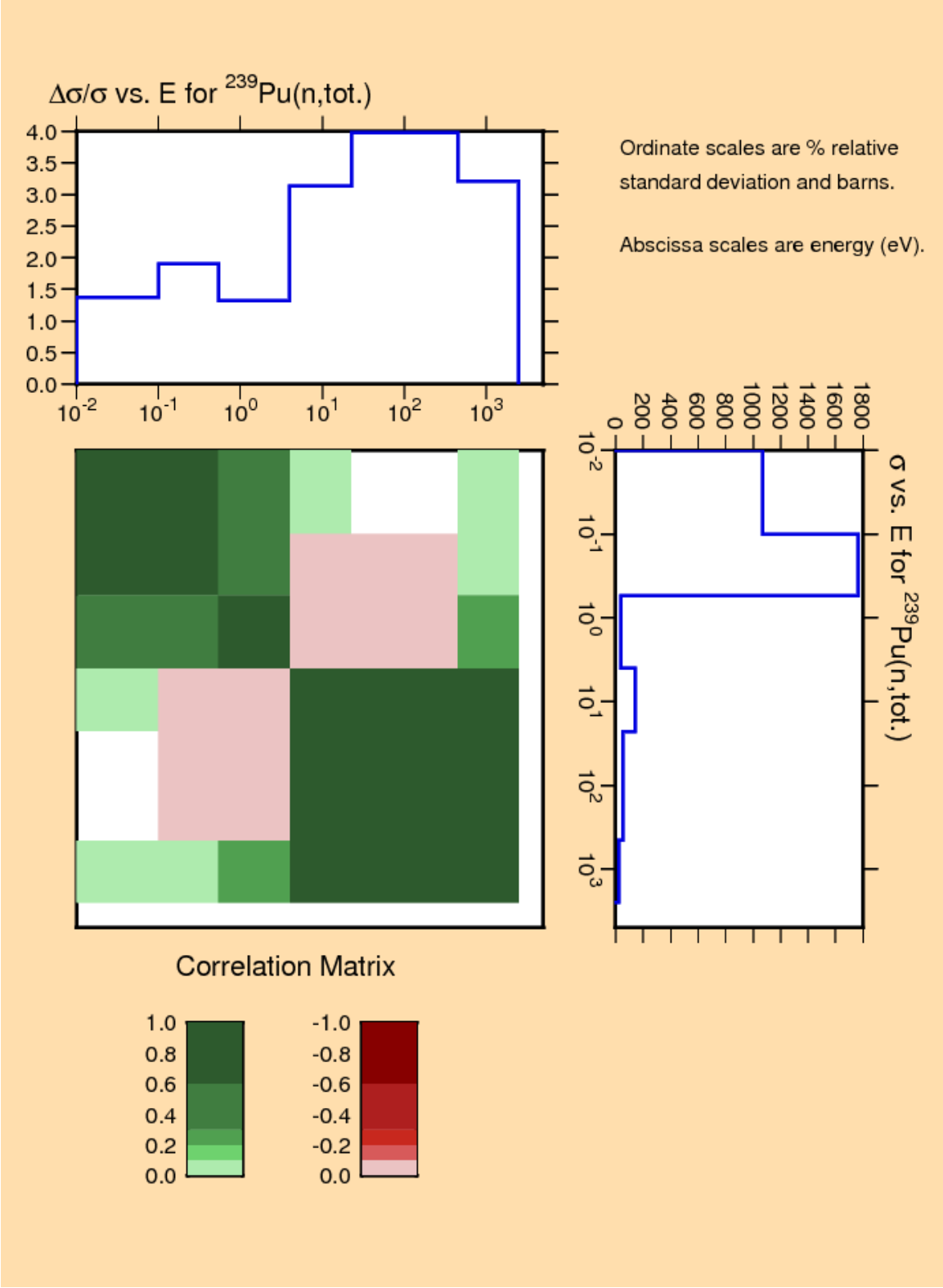

Figure 8: Relative uncertainties and correlation matrix for the total cross-section.

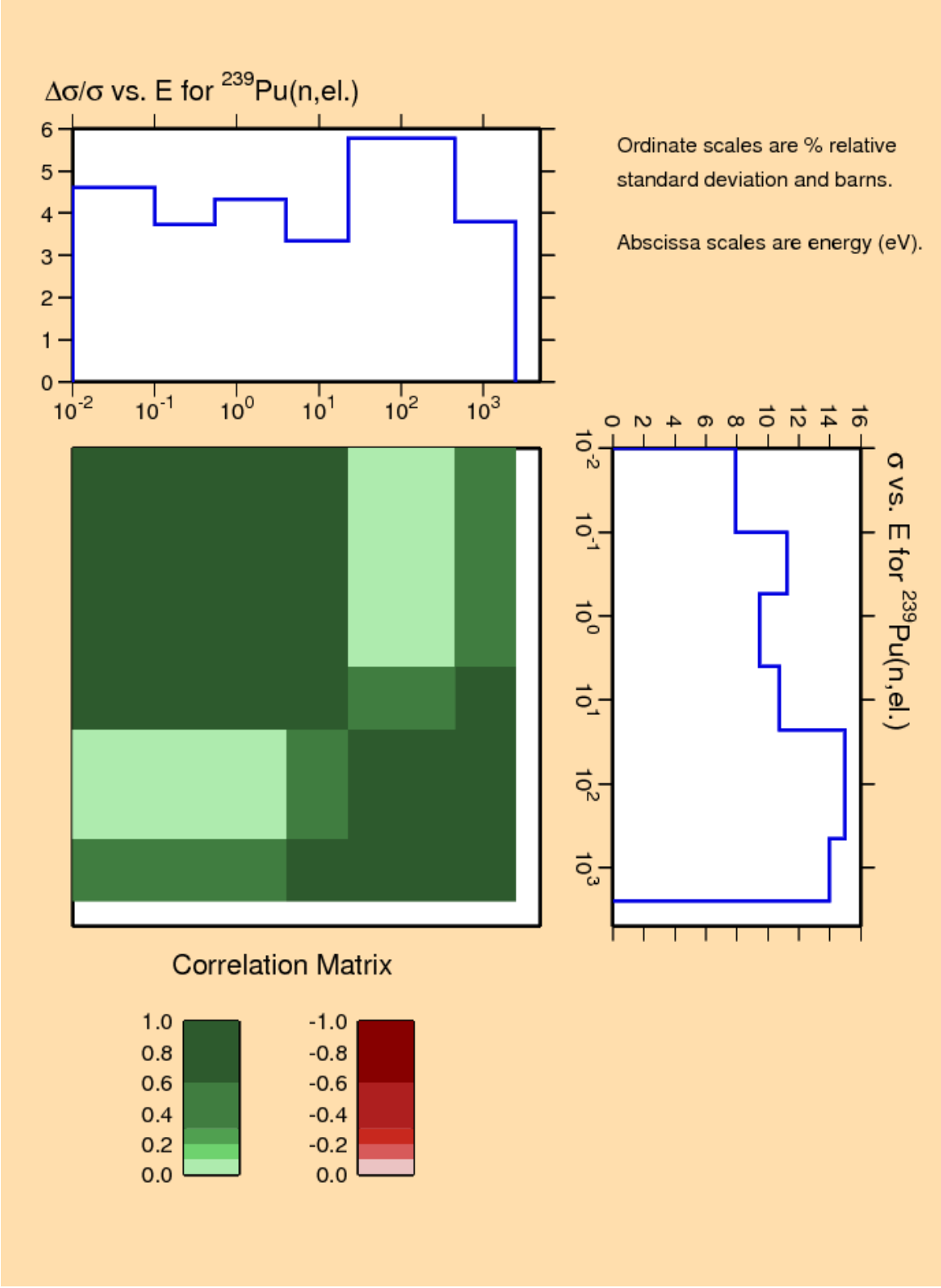

Figure 9: Relative uncertainties and correlation matrix for the elastic cross-section.

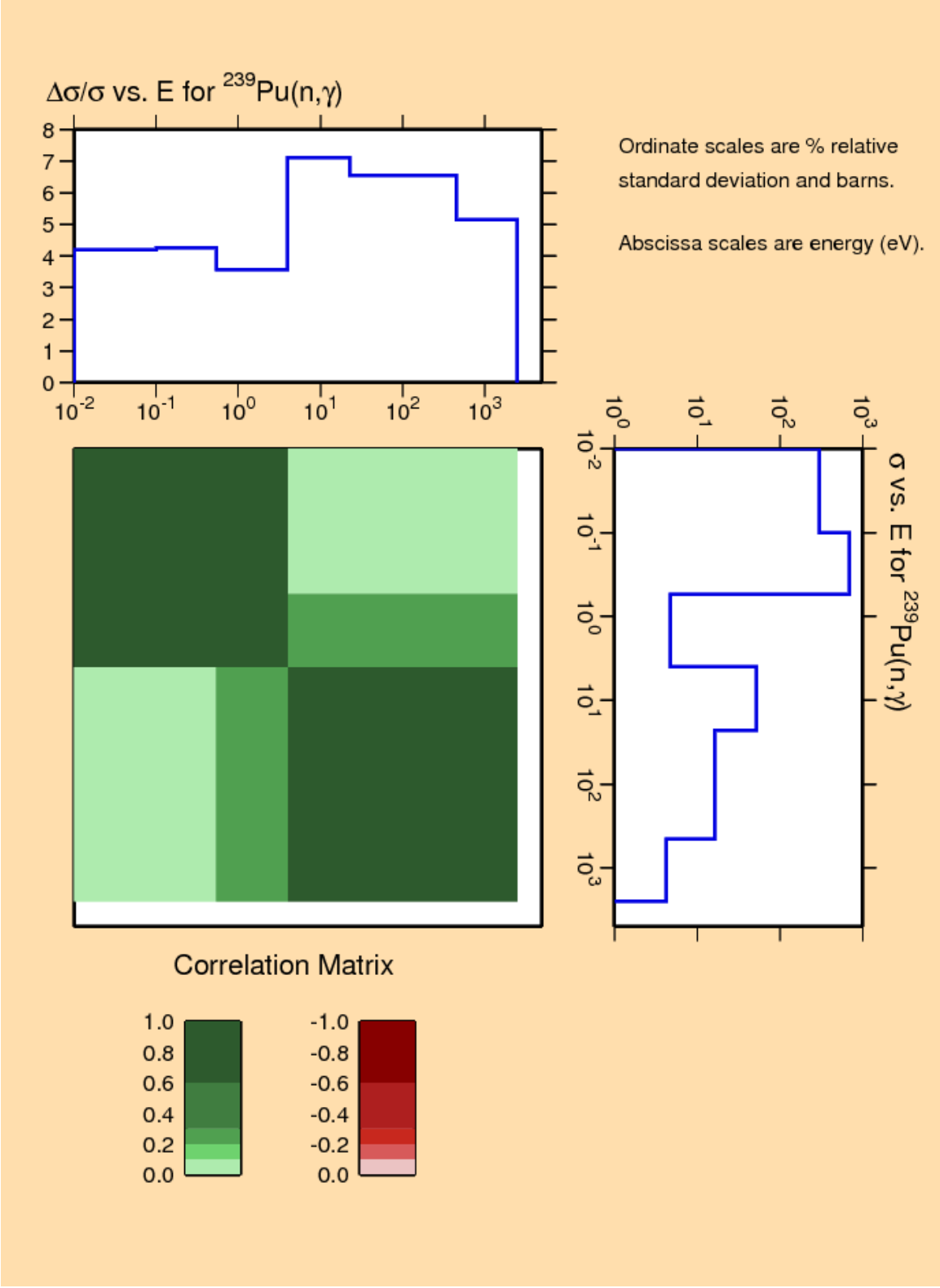

Figure 10: Relative uncertainties and correlation matrix for the capture cross-section.

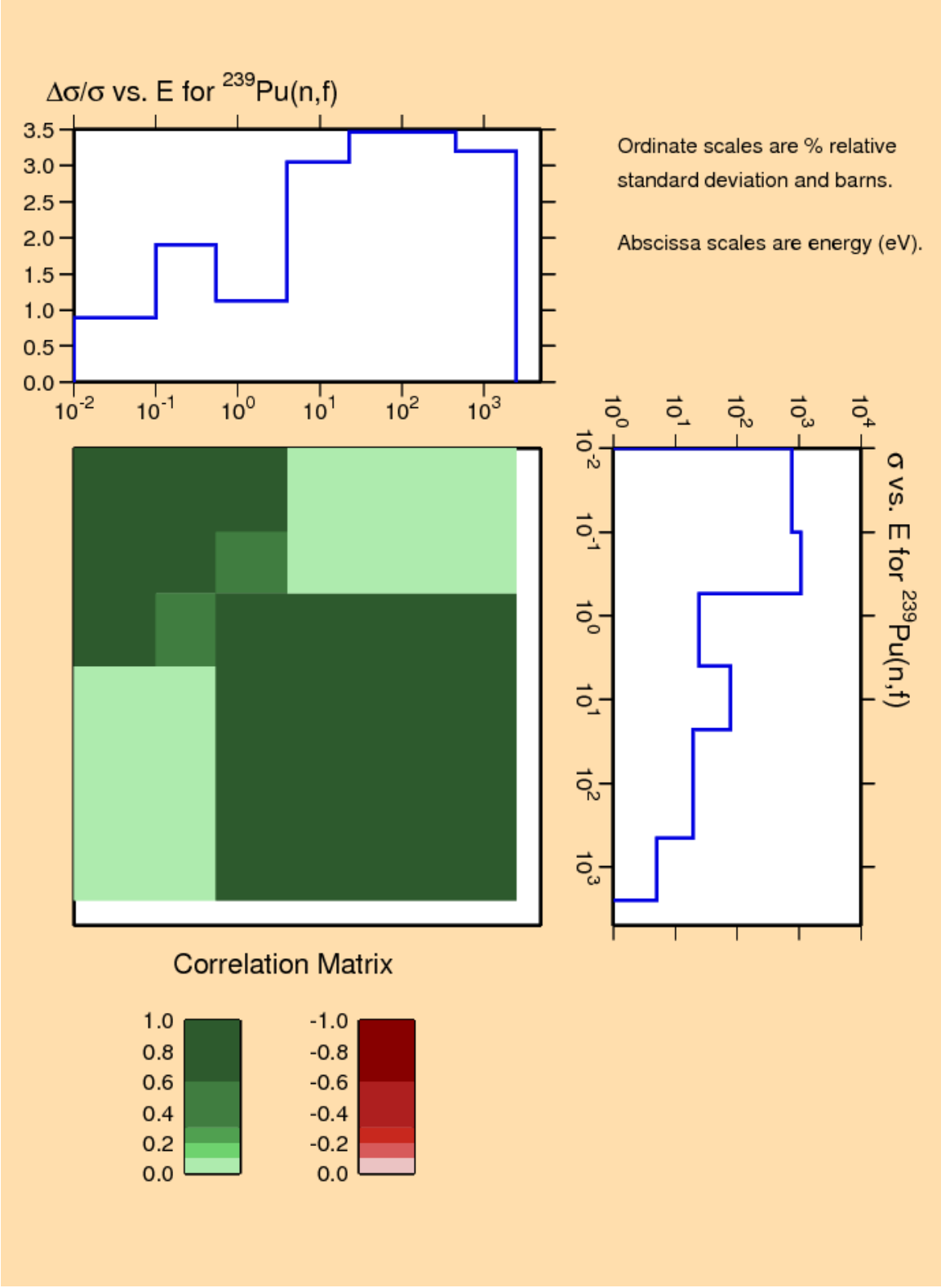

Figure 11: Relative uncertainties and correlation matrix for the fission cross-section.

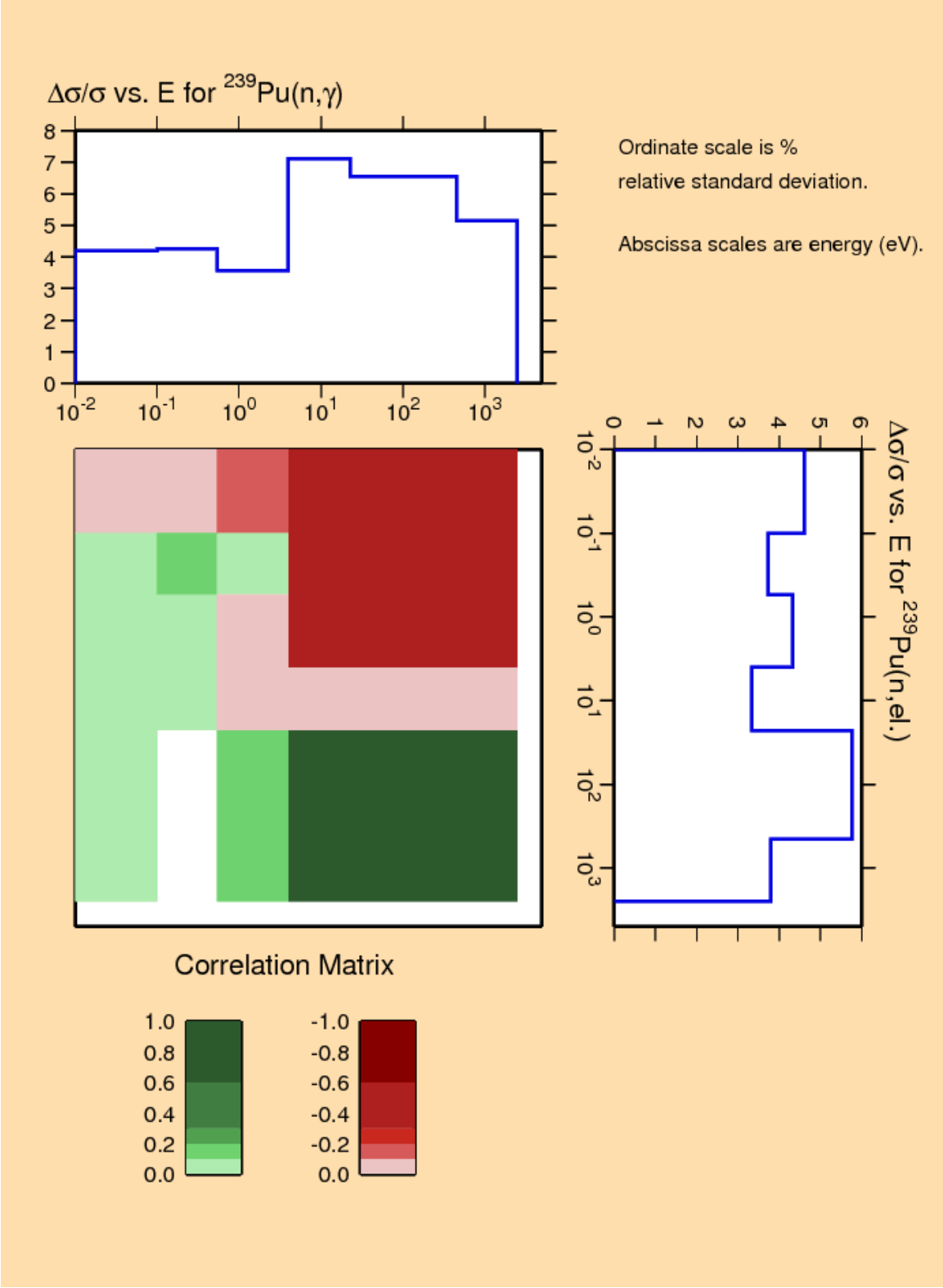

Figure 12: cross-correlation matrix between the capture and elastic cross-sections.

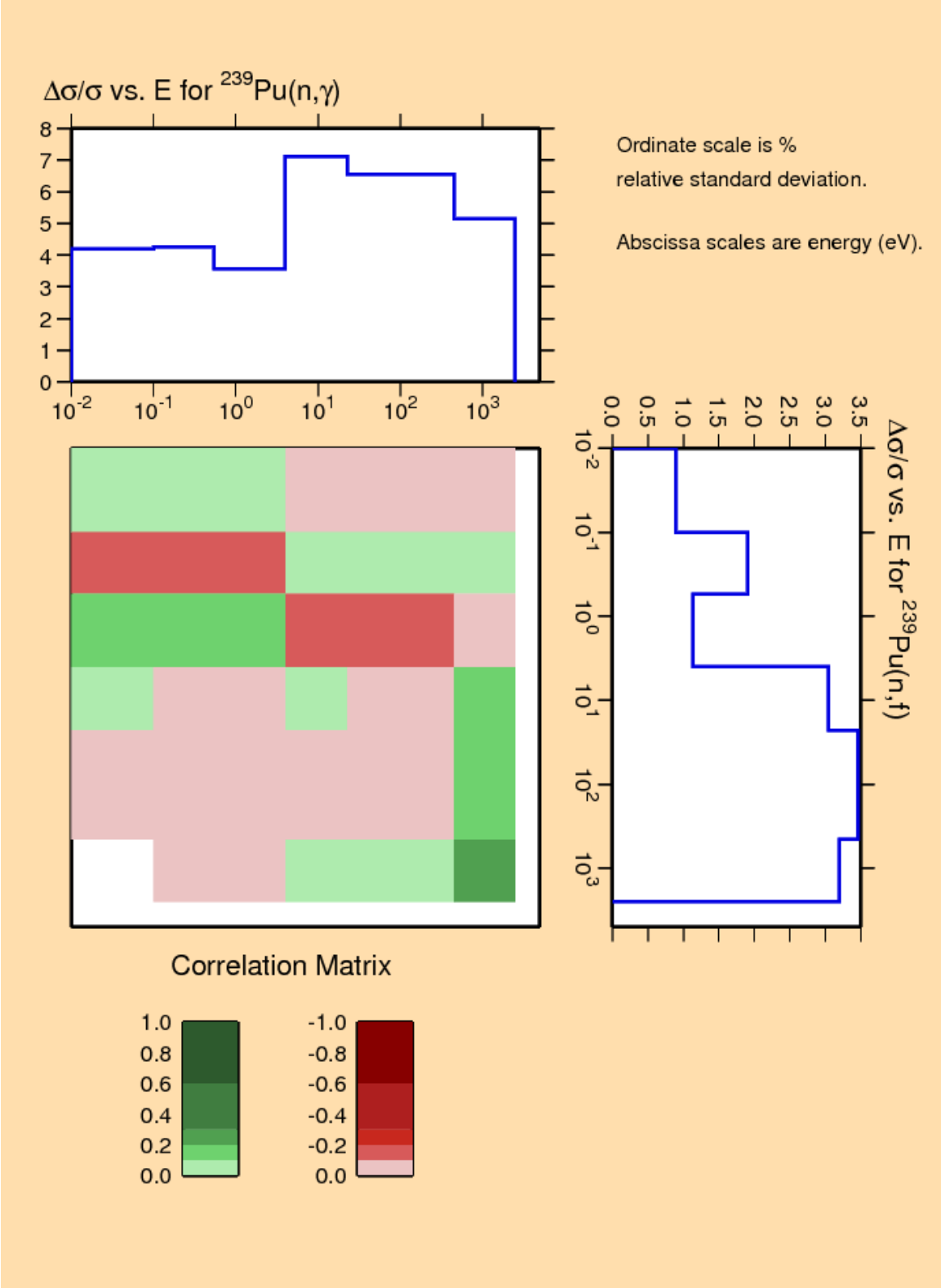

Figure 13: cross-correlation matrix between the capture and fission cross-sections.

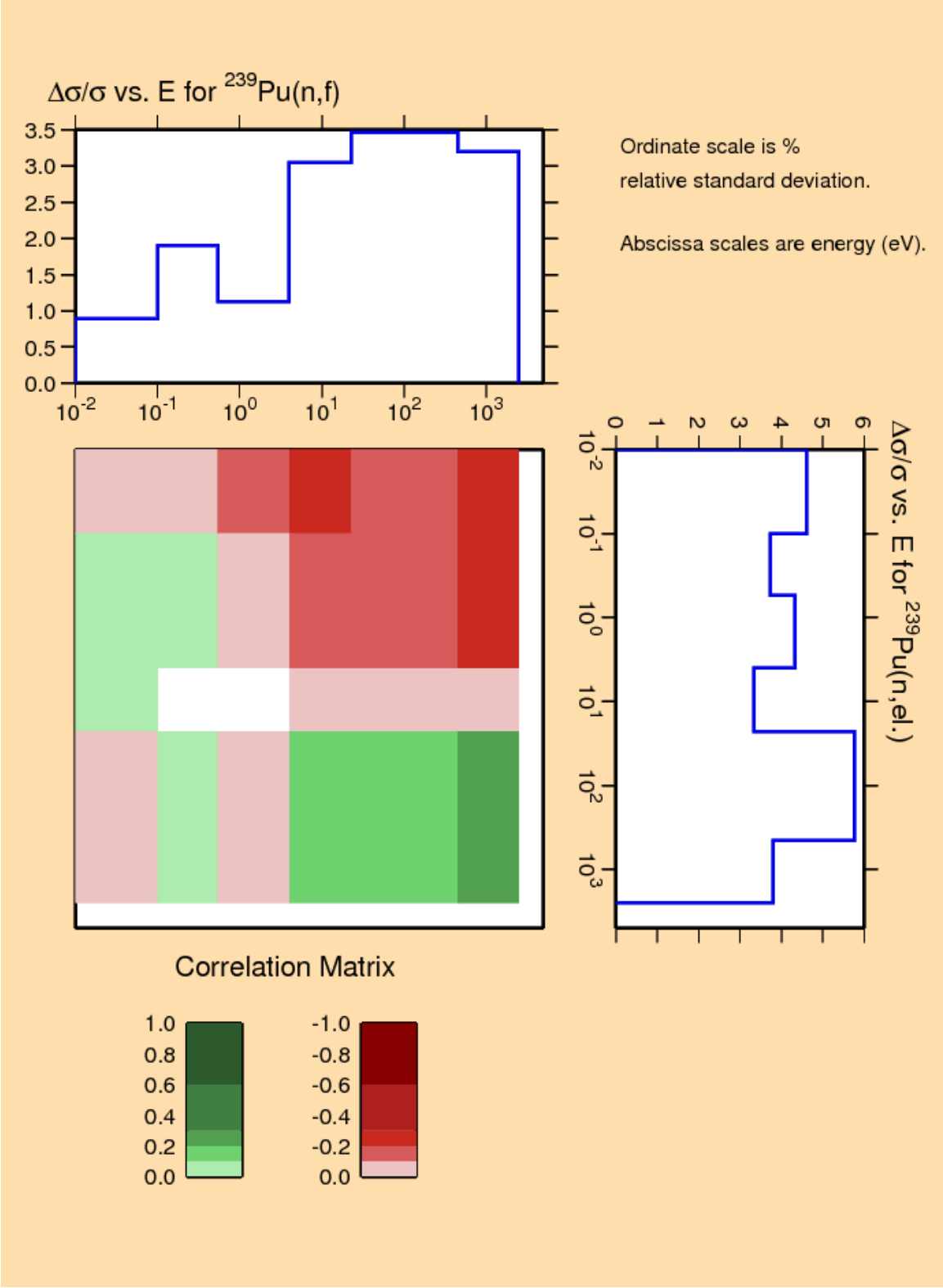

Figure 14: cross-correlation matrix between the fission and elastic cross-sections.

5. Prompt neutron multiplicity in the resonance range

Large fluctuations of the neutron multiplicity were observed in the resonance range. According to the spin assignment, the observed fluctuations are stronger for resonances having $J=1^+$. The latter channel is characterised by an average fission width of about 30 meV, while for $J=0^+$, the average fission width is close to 2 eV since the number of fission transition states involved is larger (2 to 3 compared to 1 at low energy for the other s-wave resonance spin $J=1^+$). The (n,γf) two-step reaction was introduced as a competitive reaction to explain the specific channel spin dependence observed in the prompt neutron multiplicity $\nu_p(E)$. The (n,γf) reaction and its implications are presented in this section.

5.1. Investigation of the two-step (n,γf) process

The (n,γf) process was emphasized by Lynn in 1959. The formal description of such a two-step process was published in 1965 in Reference [28] and it was recalled in 1980 in Reference [29]. Three PhD thesis performed on ^{239}Pu provide additional results about this two-step process [30-32]. However, the existence of the (n,γf) reaction is still a topic of discussion because direct measurements of this reaction are a genuine challenge.

Authors that argue the existence of the (n,γf) process assume that the observed fission is the sum of the one-step (or "direct") fission and of the two-step (n,γf) reaction:

$$\sigma_f^{obs}(E) = \sigma_f(E) + \sigma_{\gamma f}(E).$$

From a theoretical point of view, the (n,f) and (n,γf) reaction widths have to be fitted simultaneously during the Neutron Resonance Shape Analysis. Such an approach implies a modification of the resolved resonance range (RRR) formalism used in standard shape analysis codes (as SAMMY, REFIT, CONRAD…) and of the subsequent processing codes (as NJOY, CALENDF…). This work does not correspond to the present subgroup tasks. The alternative chosen in the present work was to deduce the contribution of two-step processes from the fitted Reich-Moore parameters by introducing additional J-dependent partial widths $\Gamma_{\gamma f}$. Due to the numerous intermediate states reached before second-step fission by gamma decays to be averaged over the fission transition states opened, the partial width of each spin J for the (n,γf) reaction can be assumed constant below 2.5 keV.

Figure 15 shows the contribution of this competitive reaction in the RRR and in the neutron spectroscopy continuum domain. Below 2.5 keV, we use $\Gamma_{\gamma f} = 7.3$ meV for $J=0^+$ and $\Gamma_{\gamma f} = 4.2$ meV for $J=1^+$. The magnitude of the (n,γf) contribution deduced from the resonance parameters is compared with the theoretical curve estimated with the AVXSF code [33]. The latter code has been developed at Los Alamos by Eric Lynn since the early 70's and a more robust and extensive version in Fortran 95 is now supported by CEA at Cadarache. Detailed formulae implemented in this nuclear fission data evaluation code that were in particular used for estimating the average cross-sections of the Pu family over the URR range up to 5.5 MeV, can be found in Reference [34].

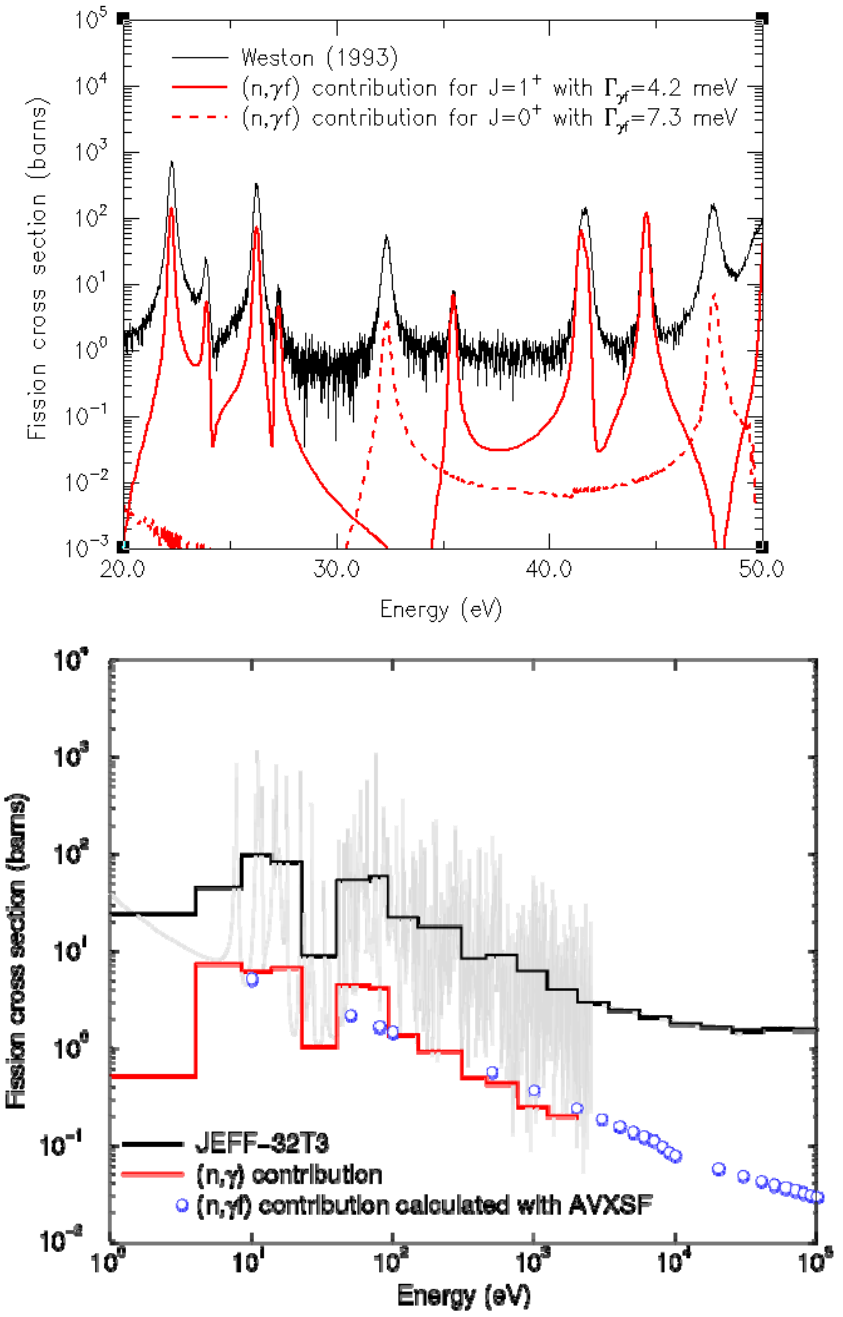

Figure 15: Comparison of both the ^{239}Pu fission cross-section and the (n,γf) reaction deduced from the resonance parameters (upper plot) and calculated with the AVXSF code (lower plot). The JEFF-3.2T2 evaluation contains the resonance parameters evaluated in the frame of this subgroup.

The upper plot of Figure 15 confirms the non-negligible contribution of the (n,γf) reaction for small s-wave resonances having $J=1^+$ because of the low one-step fission cross-section in that channel spin. Future evaluation works on ^{239}Pu will have to include explicitly the two-step (n,γf) reaction as an additional dedicated partial reaction width, $\Gamma_{\gamma f}$,

in the evaluated data file; the meaning of the usual fitted fission width becoming clear and corresponding to namely the one-step fission component only.

5.2. Study of the channel spin dependence of $\nu_p(E)$

As shown in the upper plot of Figure 15, the (n,γf) reaction may become the dominant fission contribution for small resonances characterized by an angular momentum $J=1^+$. These properties were used to explain the large fluctuations of the prompt neutron multiplicity in the resonance range since the average energy carried away by the pre-fission photon is around 1 MeV; energy amount that is not available for the neutron emission during the fission process. The emitted number of neutrons is logically reduced in proportion. In the present work, we use a phenomenological decomposition of the neutron multiplicity. This decomposition was already applied by Eric Fort to establish the neutron multiplicity file released in the JEFF-3.1 library [35]. The low energy part (below 22 eV) was modified in the JEFF-3.1.1 library for improving the k_{eff} results of various benchmarks [4]. The JEFF-3.1.1 and JEFF-3.1 multiplicities are compared in Figure 16.

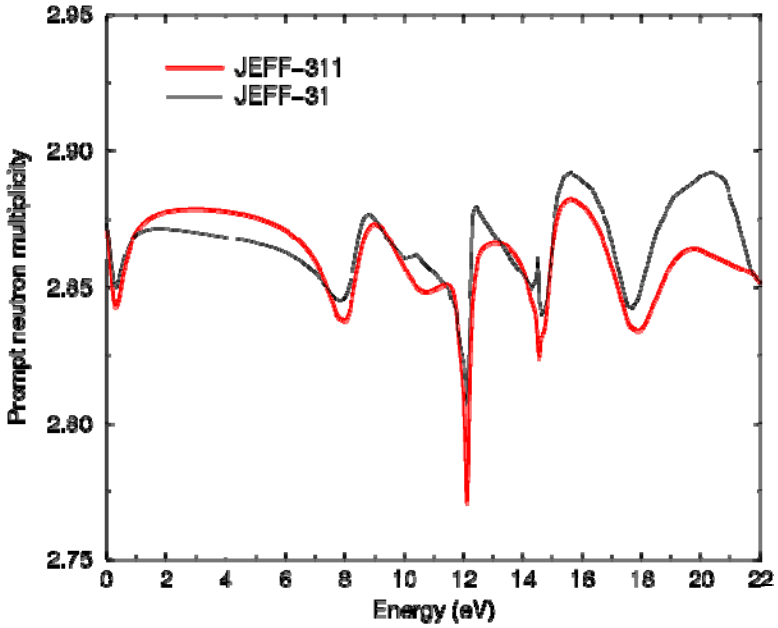

Figure 16: Comparison of the ^{239}Pu prompt neutron multiplicity available in the European libraries.

The neutron multiplicity can be viewed as the sum of four contributions due to two fission widths Γ_f and $\Gamma_{\gamma f}$ for each channel J=0 and J=1. The neutron multiplicity can be expressed as follow:

$$\nu_p(E) \approx \sum_{i=1}^{4} \nu_i P_i(E)$$

In which ν_i are free parameters and $P_i(E)$ are probabilities defined as:

$$P_i(E) = \frac{\sigma_i(E)}{\sigma_f(E) + \sigma_{\gamma f}(E)},$$

where σ_i(E) represents the partial one-step fission or (n,γf) cross-sections for a given J.

Final results are shown in Figure 17. They were obtained using the CONRAD code involving a least squared fit performed over EXFOR data [32,36]. The theoretical curve was calculated with $\Gamma_{\gamma f}$ = 7.3 meV for $J=0^+$ and $\Gamma_{\gamma f}$ = 4.2 meV for $J=1^+$.

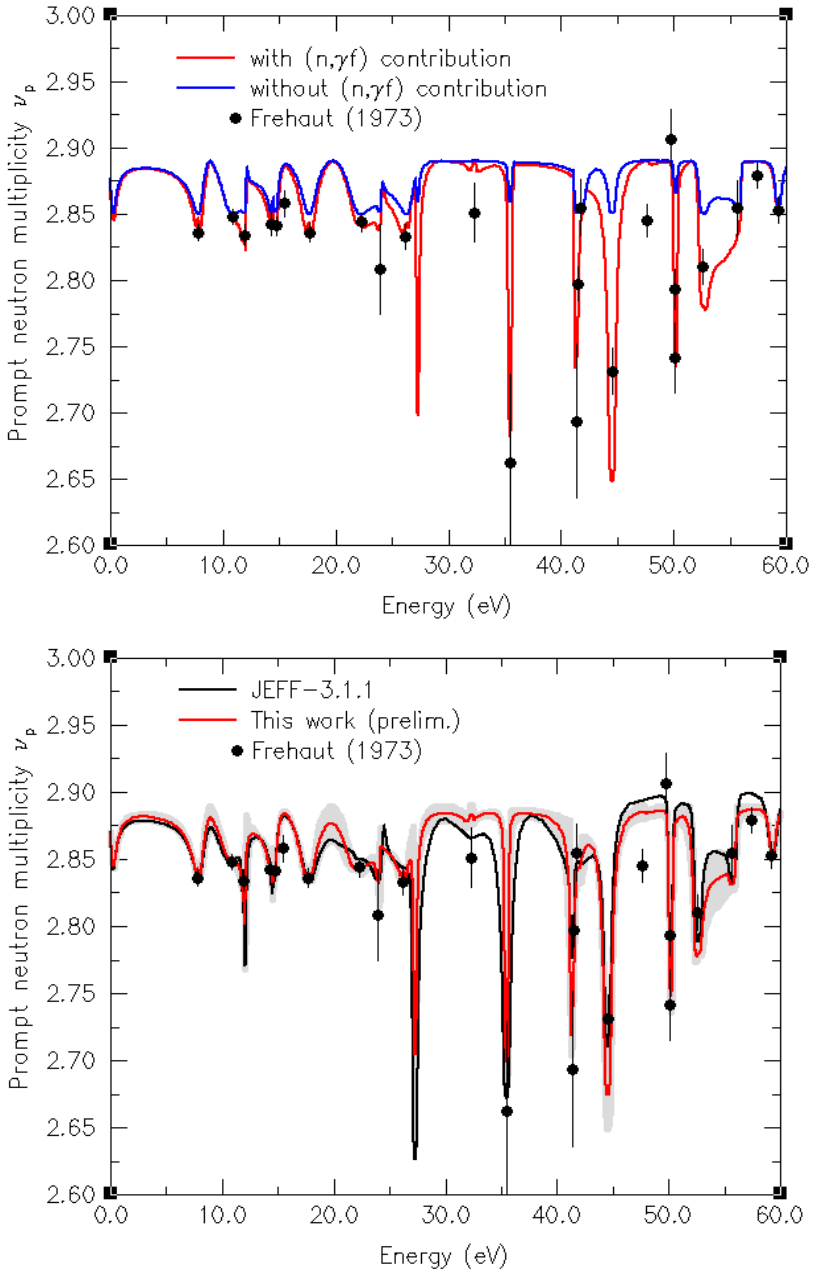

Figure 17: The upper plot represents the neutron multiplicities calculated with and without the (n,γf) process. The lower plot compares the present work with the JEFF-3.1.1 evaluation.

The upper plot compares the magnitude of the neutron multiplicity with and without the contribution of the two-step (n,γf) process. Without the (n,γf) contribution, the phenomenological description of the neutron multiplicity fails to reproduce the large variations observed for resonances having J=1. For J=0, the contribution of the (n,γf) reaction ($\Gamma_{\gamma f}$ = 7.3 meV) is negligible compared to the magnitude of the average one-step fission width as large as 2 eV.

The lower plot of Figure 17 shows that the present work is in good agreement with the JEFF-3.1.1 evaluation. The free parameters ν_i extracted by CONRAD are reported in Table 5. The CONRAD results confirm the values reported in Reference [35]. As a consequence, the neutron multiplicity energy shape in the resolved resonance range of JEFF-3.1.1 is recommended for the next ^{239}Pu evaluation.

Table 5: Values of the free parameters ν_i determined in this work and compared with those reported in Reference [35].

Reaction	J^{π}	Fort et al. (1988)	This work
(n,f)	1^+	2.86	2.85
(n,f)	0^+	2.88	2.89
(n,γf)	1^+	2.66	2.62
(n,γf)	0^+	2.80	2.62

6. Integral validation of the ^{239}Pu resolved resonance range

Preliminary MCNP calculations on seven dedicated benchmarks were continuously performed during the elaboration of the resolved resonances with the SAMMY code. Results are reported in Section 4.3.2. Additional integral results are presented in this section based on both ENDF/B-VII.1 and JEFF-3.1.1 libraries as reference, i.e. the SG34 ^{239}Pu file replaced when mentioned existing ENDF and JEFF ^{239}Pu files. The SG34 ^{239}Pu file contains new resonance parameters as well as nu-bar and (n,γf) cross-sections.

6.1. Integral validation based on JEFF-3.1.1 + SG34 ^{239}Pu

The calculations were performed with the Monte Carlo code TRIPOLI. The resolved resonances established in the frame of this subgroup were included in the latest version of the NEA library JEFF-3.1.2 (=JEFF-3.1.1). The benchmarks of interest come from the ICSBEP and CEA databases.

6.1.1. Plutonium Solution Thermal (ICSBEP)

The ICSBEP benchmarks of interest for this work are reported in Table 6. As indicated in Section 4.3.2, the benchmarks PST-001 and PST-004 consist of light water reflected spheres of plutonium nitrate solutions. The latest benchmark PST-016 has a cylindrical geometry. Results for two benchmarks (PST-001.4 and PST-004.1) were already reported in Figure 6.

The mean value of the results seems to indicate a slight improvement of 50 pcm by using the new SG34 ^{239}Pu evaluation. This improvement is probably not significant because of the large statistical error of about 30 pcm on the TRIPOLI results. Therefore, the major conclusion provided by these results is that the performances of the new ^{239}Pu evaluation will be equivalent to JEFF-3.1.1 for light water reactor applications. This conclusion is confirmed by the trends reported in Figure 6, where the red symbols are closer to the black circles obtained with the ^{239}Pu evaluation of JEFF-3.1.1.

Table 6: Integral results (in pcm) obtained with the JEFF-3.1.1 and JEFF-3.1.1+SG34 ^{239}Pu libraries with the Monte Carlo code TRIPOLI-4. The results in red correspond to the benchmarks used during the Neutron Resonance Shape Analysis (See Section 4.3.2)

Benchmarks	series	Exp. Unc.	JEFF-3.1.1	JEFF-3.1.1+SG34 ^{239}Pu	Δ(SG34-JEFF-3.1.1)
PU-SOL-THERM-001	1	± 500	181 ± 36	150 ± 35	-31
	2		399 ± 35	339 ± 36	-60
	3		725 ± 35	656 ± 35	-69
	4		**173 ± 35**	**89 ± 34**	**-84**
	5		535 ± 35	470 ± 34	-65
	6		738 ± 34	698 ± 35	-40
PU-SOL-THERM-004	**1**	± 470	**-332 ± 34**	**-333 ± 35**	**-1**
	2		-503 ± 34	-498 ± 36	+5
	3		-356 ± 34	-258 ± 34	+98
	5		-413 ± 35	-422 ± 35	-9
	6		-184 ± 35	-180 ± 35	+4
	8		-252 ± 36	-300 ± 35	-48
PU-SOL-THERM-016	1	± 430	534 ± 28	450 ± 28	-84
	2		573 ± 28	504 ± 28	-69
	3		643 ± 28	594 ± 28	-49
	4		669 ± 27	553 ± 28	-116
	5		418 ± 28	258 ± 28	-160
	6		497 ± 29	413 ± 28	-84
	7		475 ± 28	429 ± 28	-46
Mean value			+238	**+190**	-48
Standard deviation			433	398	

6.1.2. Mock-up facilities and power reactors.

The impact of the new ^{239}Pu evaluation was investigated with integral results obtained on mock-up facilities and power reactors by inserting the SG34 ^{239}Pu file in the JEFF-3.2 Test library, which also contains a new ^{241}Am evaluation in the resonance region.

The consistency of the low energy part of the fission and capture cross-sections was investigated with integral data measured in the frame of the CERES-PU programme [37]. The aim of this experimental programme was to measure the reactivity worth δρ of 12 MOX samples by the oscillation technique in the DIMPLE reactor (AEA, Winfrith). The interpretation was performed with the Monte Carlo code TRIPOLI. Two average values were deduced from the various C/E results. They are reported in Figure 18 as a function of the K1 parameter, already defined in section 4.3.1. An "experimental" value for the K1 parameter can be deduced from the variation of the reactivity worth obtained by using the

^{239}Pu evaluation of JEFF-3.1.1 and JEFF-3.2. For small variations of reactivity, we can assume that:

$$\Delta(\delta\rho) \propto \Delta(K1),$$

where $\Delta(\delta\rho)$ and $\Delta(K1)$ are calculated as follow:

$$\Delta(\delta\rho)=\delta\rho(\text{JEFF-3.1.1})-\delta\rho(\text{JEFF-3.2}),$$
$$\Delta(K1)=K1(\text{JEFF-3.1.1})-K1(\text{JEFF-3.2}).$$

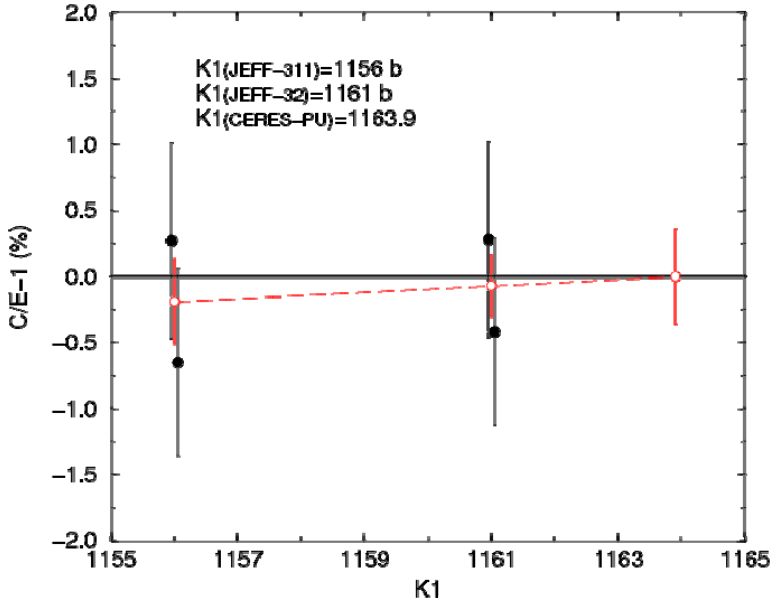

Figure 18: Average (C/E-1) results obtained from the interpretation of the CERES-PU program carried out in the DIMPLE reactor with the Monte Carlo code TRIPOLI. The results are expressed as a function of the K1 parameter.

The linear assumption between the variation of reactivity and the variation of K1 leads to an "experimental" value of 1164±15 barns. The latter is in good agreement with the K1 parameter calculated with the resonance parameters established in this work. Results are summarized in Table 7.

Table 7: Value for the K1 parameter

Data	K1 parameter
Atlas of Neutron Resonances	1177 barns
JENDL-4	1173 barns
ENDF/B-71	1166 barns
JEFF-3.1	1169 barns

JEFF-3.1.1	1156 barns
WPEC/SG34 (=JEFF-3.2)	1161 barns
This work (CERES-PU)	1164 ± 15 barns

The α ratio, meaning the ratio of the neutron-induced capture cross-section to the neutron-induced fission cross-section, was investigated in the thermal energy range via Reactivity Temperature Coefficient analysis performed with the APOLLO code on the MISTRAL-3 experiment carried out in the EOLE facility of CEA Cadarache. The analysis has shown that the negative bias reported in Table 8 for the low-temperature range (below 80°C) is linked to the thermal spectrum shift effect, which could be strongly dependent on the thermal shapes of the capture and fission cross-sections of ^{239}Pu. New APOLLO calculations with JEFF-3.2 provide a bias on the RTC close to -1.3 pcm/°C which is an intermediate result between JEFF-3.1 and JEFF-3.1.1. This result indicates that further studies on the energy dependence of the α ratio in the thermal energy range is needed.

Table 8: Bias on the Reactivity Temperature Coefficient (pcm/°C) calculated with APOLLO for the MISTRAL-3 program carried out in the EOLE facility of Cadarache.

Evaluation	**10°C-40°C**	**40°C-80°C**	**10°C-80°C**
JEFF-3.1	-2.3 ± 0.3	-0.8 ± 0.3	-1.6 ± 0.3
JEFF-3.1.1	-0.4 ± 0.5	-1.4 ± 0.5	-1.0 ± 0.4
WPEC/SG34 (=JEFF-3.2)			≈ -1.3

The latest integral validation concerns the impact of the new ^{239}Pu in fuel inventory calculations in PWR for high burn-up UOX fuels ranging from 65 GWd/t to 85 GWd/t. APOLLO results are reported in Figure 19. A slight increase of about 0.3% of the concentration of ^{239}Pu is expected. This result confirms that the performances of the new evaluation are equivalent to the ^{239}Pu evaluation of JEFF-3.1.1.

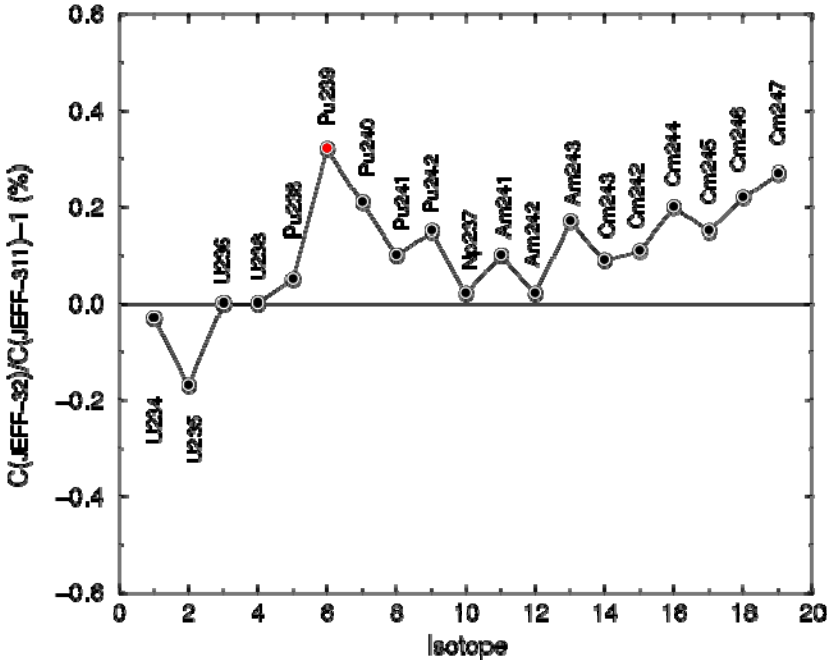

Figure 19: Fuel inventory calculations in PWR (ALIX-HBU program) for high burn-up between 65 GWd/t and 85 GWd/t. The calculations were performed with the APOLLO code. JEFF-3.2 contains this new SG34 ^{239}Pu file.

The evaluation work on ^{239}Pu was performed not only for criticality studies but also for MOX fuel applications. The new ^{239}Pu evaluation was tested on various configurations (FUBILA, MH1.2, MISTRAL) measured in the EOLE facility of CEA Cadarache. TRIPOLI and APOLLO results are reported in Figure 20. The C-E results remains below 200 pcm. For the MISTRAL experiments, the significant improvement is linked to ^{241}Am. The overall agreement demonstrates the quality of the evaluation work performed in collaboration between CEA, ORNL and IRMM on the resolved resonance range of the americium and plutonium isotopes.

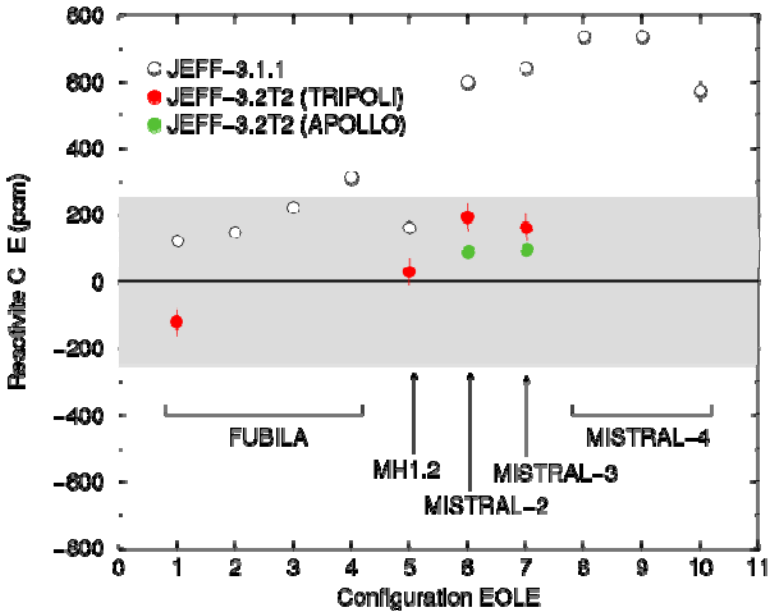

Figure 20: Residual reactivity effect obtained with JEFF-3.1.1 and JEFF-3.2 for various MOX configurations measured in the EOLE facility of CEA Cadarache. The calculations were performed with the Monte-Carlo code TRIPOLI and the deterministic code APOLLO.

6.2. Integral validation based on ENDF/B-VII.1+ SG34 ^{239}Pu

K_{eff} C/E calculations have been performed for the described subset of thermal solution benchmarks using ENDF/B-VII.1 (i). For a variety of cross-sections configurations, the ^{239}Pu data come from (ii) JEFF-3.1.2; (iii) JENDL-4.0 and (iv) SG34 activity (ORNL/CEA ^{239}Pu file developed for this study). We used ENDF/B-VII.1 cross-sections for all other nuclides in all of these calculations. The results are provided in Table 9.

Table 9: Calculated keff C/E Values

Benchmark Name	**ENDF/B-VII.1 (i)**	**JEFF-3.1.2 (ii)**	**JENDL-4.0 (iii)**	**SG34 (iv)**
PST1.4	1.00500(13)	1.00127(6)	1.00588(6)	1.00199(6)
PST4.1	1.00389(11)	0.99907(5)	1.00482(5)	1.00044(5)
PST9	1.01939(5)	1.01367(2)	1.02510(3)	1.01543(2)
PST12.10	1.00402(10)	0.99973(5)	1.00498(3)	1.00083(5)
PST12.13	1.00970(6)	1.00468(3)	1.01069(3)	1.00611(3)
PST18.6	1.00462(11)	1.00153(5)	1.00557(5)	1.00202(5)
PST34.4	1.00254(11)	0.99999(5)	1.00417(5)	0.99922(5)
PST34.15	0.99731(10)	0.99563(5)	0.99844(5)	0.99679(5)
8 assembly average	**1.00581**	**1.00195**	**1.00746**	**1.00285**

The most direct comparison of these results that demonstrates the improvements from this study is to compare the ENDF/B-VII.1 (i) column and the SG34 (iv) column; as only the ^{239}Pu data differ. The average improvement is nearly 300 pcm, or about 50% of the bias.

The primary differences in the ORNL/CEA file over that in ENDF/B-VII.1 include (i) new resolved resonance parameters, (ii) a revised prompt ν(E) below 650 eV; and (iii) a revised prompt fission neutron spectrum (PFNS). The latter two differences reflect the use of data from the JEFF-3.1.2 evaluation.

Additional calculations have been performed in which (i) only the revised resolved resonance parameters were inserted into the ENDF/B-VII.1 file, and (ii) both the revised resolved resonance parameters and the revised prompt ν(E) up to 650 eV were inserted into the ENDF/B-VII.1 file. With the RR parameter only change the 8 assembly average is 1.00495; with both RR parameters and prompt ν(E) changed the 8 assembly average is 1.00295. These results suggest that of the ~300 pcm shift noted above, about 1/3 of it is attributable to the revised resolved resonance parameters and about 2/3 of it is due to prompt ν(E).

In summary, the ^{239}Pu data file produced by this Subgroup yields improved k_{eff} C/E results compared to those from the ENDF/B-VII.1 and JENDL-4.0 files, but consistent use of ENDF/B-VII.1 data for all other nuclides masks possible improvement for the JEFF community (as seen in previous chapter: *Integral validation based on JEFF-3.1.1 + SG34 ^{239}Pu*). There are three major changes in this file compared to that found in the ENDF/B-VII.1 file, including (i) revised resolved resonance parameters, (ii) revised prompt ν(E) and (iii) revised PFNS. The majority of the observed k_{eff} C/E improvement is due to the first two of these changes.

7. Investigation on the prompt neutron fission spectrum of the ^{239}Pu

The prompt fission neutron spectra (PFNS) are crucial parameters in neutronic calculations. They are actually very important either for eigenvalue calculations, or for radiation shielding calculations because deep penetrating neutrons are born in the fast energy range and any change may have large effects on neutron flux far from the source.
The international evaluation files use the same theoretical model in general. But some very different spectra are proposed by other evaluators. The aim of this study is to evaluate the impact of these kinds of spectrum for ^{239}Pu on some typical benchmarks. The calculations are performed using the Monte Carlo transport code TRIPOLI-4. The considered benchmarks are taken from international databases (ICSBEP, IRPhEP) or MASURCA and EOLE French CEA mockup experimental devices.

In the first section, we present graphical comparisons or mathematical characterizations of the different spectra. Then, the TRIPOLI-4 k_{eff} calculation results with all considered spectra are presented. Finally, an analysis is proposed for some particular thermal cases for which one of the spectra has large effects.

7.1. Different ^{239}Pu spectra (PFNS)

A set of different spectra has been studied. The general principle of this study is to use the JEFF-3.1.1 library as a reference, and to replace in the ^{239}Pu evaluation file the original prompt neutron fission spectra by JENDL-4.0, ENDF/B-VII.0, Maslov and Kornilov spectra [38-40].

As a first consideration, it has to be noticed that all international evaluations use a Madland-Nix model to get the final tabulated prompt spectra. They don't use exactly the same parameters (number of chance of fission for example) and some improvements are added (fragments kinetic energy distribution for example). These spectra are very similar. On the contrary, Maslov and Kornilov spectra are very different and are based on systematics. All the spectra are presented in Figure 21. They are compared to a Maxwellian distribution with temperature equivalent to 1.3719 MeV.

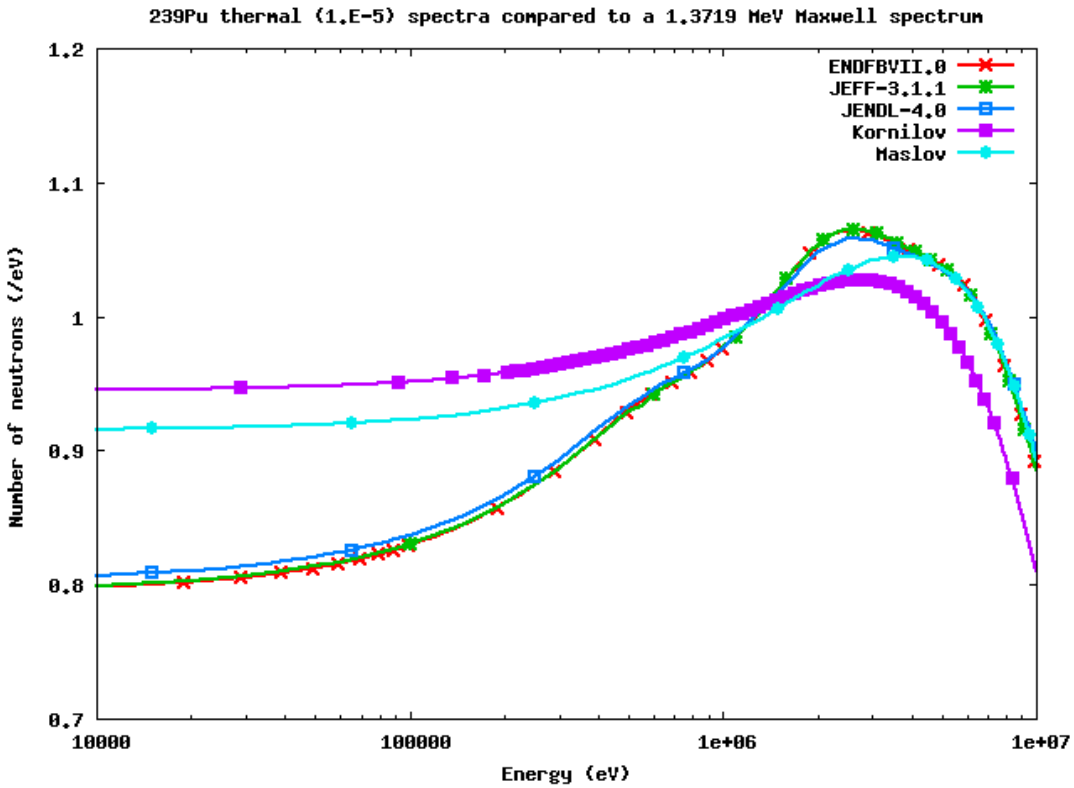

Figure 21: Kornilov spectrum, Maslov spectrum and other international evaluation file spectra compared to a Maxwellian distribution

The spectra are characterized by their mathematical moments:

$$\mu_n = \int E^n \chi(E) dE$$

First moments (mean energy) are shown in Table 10 for different incident neutron energies. The mean energy discrepancy between Kornilov spectrum and JEFF-3.1.1 one is about -2.7% at 10^{-11} MeV and -2.4% at 2 MeV. In Maslov's case, the discrepancy equals -1.0% and -0.8% at these energies, whereas the maximum discrepancy between all international evaluations are 0.2% (at 10^{-11} MeV) and 0.2% (at 2 MeV). In the following sections, only JEFF-3.1.1 spectra are compared to Maslov and Kornilov ones because all evaluations file spectra (ENDF/B, JEFF, JENDL) give very close results.

Table 10: First moment of energy distributions for all spectra

Energy (MeV)	10^{-11}	10^{-1}	1	2	5
ENDF/B-VII.0	2.112		2.138	2.163	2.236
JEFF-3.1.1	2.112	2.115	2.140	2.168	2.226
JENDL-4.0	2.116	2.122	2.140	2.165	2.237
Maslov	2.092		2.122	2.152	2.242
Kornilov	2.055		2.084	2.115	2.205

7.2. Fast, intermediate and thermal flux experiments

All the presented experiments are characterized by the EALF parameter (Energy of Average Lethargy of Fission).

7.2.1. Fast flux spectrum cases

Some fast flux criticality experiments taken in the ICSBEP database have been simulated. They all belong to the PU-MET-FAST class (Plutonium, Metal, Fast spectrum). The results are shown in Table 11. The effect between Maslov or Kornilov spectra and JEFF-3.1.1 spectra has been calculated. EALF is expressed in MeV.

Table 11: Criticality fast spectrum experiments – Difference between Maslov, Kornilov and JEFF-3.1.1 calculations

Experiment	EALF (eV)	JEFF-3.1.1 k_{eff}	Maslov (Δ, pcm)	Kornilov (Δ, pcm)
PMF001	1.330	1.00046 (12)	-114 (17)	-279 (17)
PMF002	1.330	1.00433 (5)	-116 (7)	-271 (7)
PMF011	0.108	0.99707 (15)	+41 (21)	-17 (21)
PMF022	1.310	0.99810 (7)	-91 (10)	-227 (10)
PMF024	0.699	0.99982 (8)	-4 (10)	-104 (11)
PMF027	0.090	1.00131 (8)	+10 (11)	+0 (11)
PMF029	1.330	0.99747 (7)	-113 (10)	-264 (10)
PMF031	0.223	1.00333 (8)	-1 (11)	-63 (11)

The fast spectrum mockup cases are either taken in IRPhEP database or in MASURCA experimental program. The considered IRPhEP experiments are the SNEAK7A and SNEAK7B, and the MASURCA results are coming either from CIRANO Pu burning cores program (ZONA 2A, 2B or 2A3 experiments) or from PRE-RACINE program dedicated to Super-Phenix reactor (PRE-RACINE I, IIA or IIB experiments). See Table 12.

Table 12: Mockup fast spectrum experiments – Difference between Maslov, Kornilov and JEFF-3.1.1 calculations

Experiment	EALF (eV)	JEFF-3.1.1 k_{eff}	Maslov (Δ, pcm)	Kornilov (Δ, pcm)
ZONA2A	0.192	1.00995 (12)	-149 (17)	-310 (17)
ZONA2B	0.117	1.00918 (3)	-148 (4)	-308 (4)
ZONA2A3	0.142	1.01034 (12)	-140 (17)	-282 (17)

PRE-RAC. I	0.085	1.00446 (12)	-67 (17)	-112 (17)
PRE-RAC. IIa	0.089	1.00431 (12)	-74 (17)	-145 (17)
PRE-RAC. IIb	0.094	1.00409 (12)	-57 (17)	-157 (17)
SNEAK7A	0.135	1.01001 (2)	-123 (3)	-285 (3)
SNEAK7B	0.141	1.00466 (2)	-181 (3)	-390 (3)

As expected, the effect is larger for Kornilov spectra and is negative. Actually, the sensitivity calculations performed with the deterministic system ERANOS/PARIS [41] explain this large effect. The sensitivity to high energy (1 MeV and more) is very important and changes in this energy range have a large impact on k_{eff} (see Figure 22).

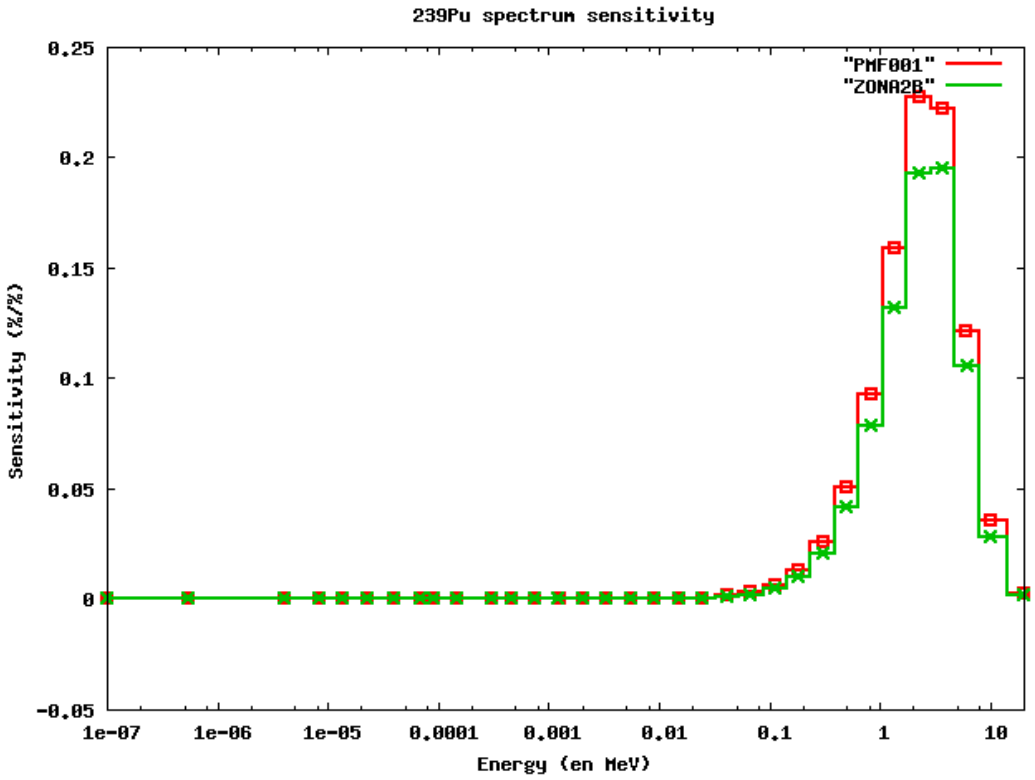

Figure 22 k_{eff} sensitivities on spectrum for ZONA2B and PU-MET-FAST 001 fast flux spectrum experiments

7.2.2. Intermediate flux spectrum cases

The intermediate flux spectrum experiments PU-COMP-INTER-001 (HISS experiments in Hector reactor), PU-MET-INTER-002 (ZPR-6 assembly 10) and PU-MET-MIXED-001 (or BFS-81 experiment) EALF values cover the energy range from 1 eV to 10 keV. In Table 13, EALF is given in eV.

Table 13: Criticality intermediate spectrum experiments - Difference between Maslov, Kornilov and JEFF-3.1.1 calculations

Experiment	EALF (eV)	JEFF-3.1.1 k_{eff}	Maslov (Δ, pcm)	Kornilov (Δ, pcm)
PCI001	319	1.00860 (11)	-56 (16)	-99 (16)
PMI002	10200	1.03234 (13)	+61 (18)	+85 (18)
PMM001-1	5540	1.00510 (35)	+108 (50)	+200 (49)
PMM001-2	276	1.00470 (20)	+91 (33)	+271 (28)
PMM001-3	61.4	1.00590 (19)	+161 (27)	+332 (29)
PMM001-4	1.34	1.00770 (20)	+98 (29)	+321 (28)
PMM001-5	1.29	1.00719 (19)	106 (26)	+326 (25)

The effect is positive this time. For the PCI case, the effect is negative. The experiment corresponds to a k_∞ "measurement" and the leakage effect analyzed in the previous section does not occur in this case.

7.2.3. Thermal flux spectrum cases

The thermal flux spectrum experiments come either from the ICSBEP database and particularly from the PU-SOL-THERM class (Plutonium, Solution, Thermal spectrum) or from the EOLE French mockup experimental program (MISTRAL 100% MOX high moderation core experiments). Results are given in Table 14. The effect of PFNS on PU-SOL-THERM 001, 004, 005, 006 and 007 is very important when using the Kornilov spectrum. This huge effect is due to large leakage. Some other explanations will be given in the next section. For other cases, the discrepancy is much lower.

Table 14: Criticality thermal spectrum experiments - Difference between Maslov, Kornilov and JEFF-3.1.1 calculations

Experiment	EALF (eV)	JEFF-3.1.1 k_{eff}	Maslov (Δ, pcm)	Kornilov (Δ, pcm)
PST001-1	0.089	1.00106 (10)	+411 (14)	+876 (14)
PST001-4	0.154	1.00041 (14)	+394 (20)	+880 (20)
PST001-6	0.367	1.00642 (10)	+366 (14)	+822 (14)
PST004-5	0.054	0.99594 (10)	+328 (14)	+737 (14)
PST005-1	0.055	0.99862 (10)	+318 (14)	+729 (14)
PST005-7	0.068	1.00052 (10)	+318 (14)	+757 (14)
PST006-2	0.053	0.99827 (10)	+294 (14)	+668 (14)
PST007-3	0.272	1.00095 (10)	+373 (14)	+843 (14)
PST007-10	0.107	0.99743 (10)	+388 (14)	+867 (14)
PST012-5	0.043	1.00974 (10)	+54 (12)	+155 (14)
PST012-13	0.043	1.00594 (10)	+50 (14)	+173 (14)

For EOLE mockup experiments (see Table 15), the impact of the Kornilov and Maslov spectra is less important. Although leakage is quite important in these configurations, the fissile material is different (MOX fuel). The fast neutron fissions effect contributes to the reduction of the discrepancies (see factor ε in next section).

Table 15: EOLE mockup thermal spectrum experiments - Difference between Maslov, Kornilov and JEFF-3.1.1 calculations

Experiment	JEFF-3.1.1 k_{eff}	Maslov (Δ, pcm)	Kornilov (Δ, pcm)
MISTRAL-2	1.00726 (4)	+37 (6)	+74 (6)
MISTRAL-3	1.00767 (4)	+54 (6)	+110 (6)

7.2.4. Physical analysis

An analysis has been performed to understand the huge effect of Kornilov spectrum in some thermal flux cases. The analysis is based on k_{eff} and k_∞ expressions. k_∞ can be written by the well-known Fermi's formula:

$$k_\infty = \varepsilon.p.f.\eta$$

where ε is the fast energy range amplification factor, p is the probability to escape to absorption in epithermal energy range, f is the probability to be absorbed in the fissile zones in the thermal energy range, η is the mean number of fission neutrons per thermal absorption.

$$k_{eff} = k_\infty/(1 + M^2 B^2),$$

where M^2 is the migration area, B^2 is the buckling. Table 16 shows each of these factors (plus ν, the number of neutrons per fission) in the case of JEFF-3.1.1 PFNS and Kornilov PFNS for PU-SOL-THERM-001 case 1.

Table 16: PU-SOL-THERM-001 k_∞ - JEFF-3.1.1 versus Kornilov calculations expressed in PCM

Factor	JEFF-3.1.1 k_{eff}	Kornilov (Δ, pcm)
ε	1.06448 (13)	-14 (13)
p	0.89366 (1)	+29 (1)
f	0.91994 (12)	0 (11)
ν	2.86787 (34)	-6 (34)
η	1.92387 (12)	-3 (12)
k_∞	1.68364 (32)	+28 (31)

The table shows that all the k_∞ factors (as well as k_∞ itself) are very close. In Figure 23, the fissile zone outgoing net current discrepancy between the two calculation cases is plotted. For the PU-SOL-THERM-001 case, more neutrons leave the fission zone with the JEFF-3.1.1 spectrum and are absorbed in the water reflector. As long as B^2 does not change, the reactivity effect is due to migration area change. This can be explained by the decrease of the ^1H elastic cross-section above 1 MeV. Actually, the decrease of the mean neutron energy with Kornilov spectrum leads to an increase of this averaged cross-section, and consequently a decrease of the migration area.

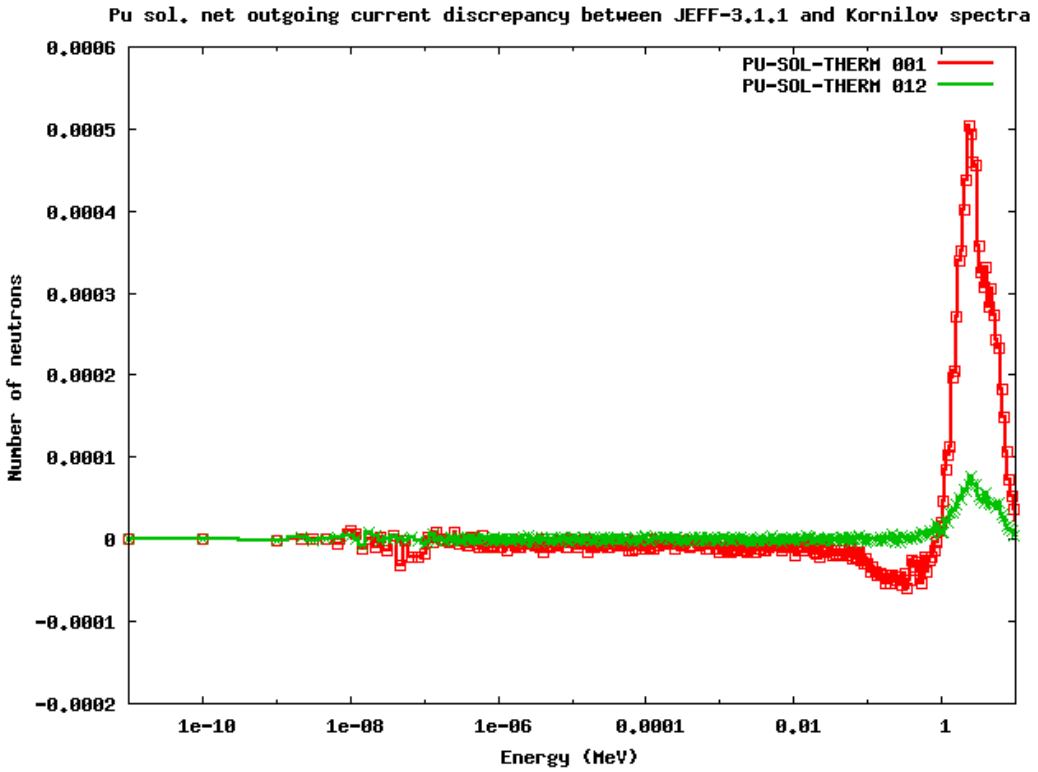

Figure 23: Fissile zone outgoing net current discrepancy between JEFF-3.1.1 and Kornilov spectra calculations

7.3. Summary of the PFNS study

This work has shown that the Prompt Fission Neutron Spectra in ENDF/B-VII.0, JEFF-3.1.1 and JENDL-4.0 are very close to each other and that the calculated effective multiplication factors on a set of selected benchmarks are slightly affected by these different evaluations. On the contrary, the Maslov and Kornilov spectra may have huge effect for some particular configurations. In particular, the calculated impact on the effective multiplication factor can reach +800 pcm in PU-SOL-THERM experiments (with high leakage level) and -300 pcm in fast spectrum experiments, either for ICSBEP benchmarks or CEA/MASURCA mockup benchmarks.

8. Conclusions

The international effort performed in the frame of this Subgroup allowed to deliverer a single set of resonance parameters up to 2.5 keV able to provide good C/E results over a broad set of integral data. The resonance analysis was performed with the SAMMY code. The thermal capture and fission cross-sections are 270 ± 11 barns and 747 ± 7 barns, respectively. The quoted uncertainties were determined by marginalization with the CONRAD code. The value of the K1 parameter calculated with the NJOY processing system is 1161 barns.

The large fluctuations of the prompt neutron multiplicities were correctly reproduced with a phenomenological decomposition of the multiplicity that involved the one-step (or direct) fission reaction and the two-step (n,γf) process. Below 2.5 keV, the (n,γf) process was calculated by introducing two additional partial widths ($\Gamma_{\gamma f} = 2.8 \pm 9.2$ meV for $J=0^+$ and $\Gamma_{\gamma f} = 1.9 \pm 0.8$ meV for $J=1^+$). The final result was in good agreement with the prompt neutron multiplicity of JEFF-3.1.1.

Performances of the new ^{239}Pu evaluation were tested over a broad set of integral data (ICSBEP, mock-up experiments performed in the CEA facilities and in power reactors). An overall good agreement was achieved between the calculations and the experimental results. The performances are nearly similar to those of the ^{239}Pu evaluation of JEFF-3.1.1. More integral feedback will be obtained via the NEA WPEC Subgroups 39 and 40.

9. Proposals

The present results allow identifying several priorities for future experimental and evaluation works.

For the resolved resonance range, new transmission measurements of the 1st broad s-wave resonance at 0.3 eV are needed as well as capture yield over a large energy range. At low energy, the SAMMY/CONRAD analysis relies on a single transmission data set measured by Bollinger in 1958. For the capture cross-section the available data set, was measured by Gwin in 1971. High resolution measurements of the neutron multiplicity are also required.

Two problems occur during the evaluation work. The first one concerns the Resonance Parameter Covariance Matrix. A concise method for storing and communicating large RPCM is needed. In the present work, an artificial reduced neutron width selection was used to reduce the size of the matrix. The restrictions of the ENDF-6 format are no longer compatible with the possibilities offer by the AGS format developed at the IRMM. The second problem is related to the (n,γf) reaction and the modelling of the fluctuations of the prompt neutron multiplicity. The partial widths associated to the (n,γf) reaction have to be included in the evaluated file in order to make possible "on-the-fly" calculations of $\nu_p(E)$ for a given temperature.

In addition, some work could be proposed to connect properly the unresolved resonance range with the continuum for the evaluation of cross-sections and model parameters as well as for covariance estimation.

10. References

[1] OECD/NEA, International Handbook of Evaluated Criticality Safety Benchmark Experiments, NEA/NSC/DOC(95)03 (Rev. September 2013).

[2] F.B. Brown et al., *"Advances in the Development and Verification of MCNP5 and MCNP6"*, International Conference on Nuclear Criticality, Edinburgh, Scotland, 19-22 September 2011.

[3] D. Bernard et al., Improvements of the ^{239}Pu Evaluation for JEFF-3,JEF/DOC-1158, 2006.

[4] S. van der Marck, Criticality Safety benchmark calculations with MCNP-4C3 using JEFF-3.1 nuclear data, JEFF document JEF/DOC-1107, 2005.

[5] A. Santamarina et al., The JEFF-3.1.1 Nuclear Data Library - Validation results from JEF-2.2 to JEFF-3.1.1, JEFF Report 22, 2009.

[6] S.C. van der Marck, "Benchmarking ENDF/B-VII.1, JENDL-4.0 and JEFF-3.1.1 with MCNP6," Nuclear Data Sheets 113 (2012) 2935.

[7] N.M. Larson, ORNL0TM-91790R7, Oak Ridge National Laboratory, 2006.

[8] R.E. MacFarlane and D.W. Muir, Los Alamos National Laboratory; http://t2.lanl.gov/nis/codes/njoy99.

[9] M. Coste-Delclaux et al., "*GALILÉE: A nuclear data processing system for transport, depletion and shielding codes*", WONDER 2009 (Workshop On Nuclear Data Evaluation for Reactor applications), Cadarache, France, 2009.

[10] F. Malvagi et al., Overview of TRIPOLI4 Version 7 Continuous-energy Monte Carlo Transport Code, Proceedings of ICMPP 2011 (2011).

[11] R. Sanchez et al., "Apollo2 year 2010", Nuclear Engineering and Technology, Vol.42 No.5 October 2010.

[12] H. Derrien, G. De Saussure, and R.B. Perez, Nucl. Sci. Eng. 106 (1990) 434.

[13] H. Derrien, J. Nucl. Sci. Technol. 30 (1993) 845.

[14] J.A. Harvey et al., Proc. Int. Conf. Nuclear Data for Science and Technology, Mito, Japan May 30-June 3, 1988.

[15] H. Derrien, L.C. Leal, and N.M. Larson, "Neutron Resonance Parameters and Covariance Matrix of ^{239}Pu," ORNL/TM-2008/123, September 2008.

[16] D. Bernard et al.,"^{239}Pu Nuclear Data Improvements in Thermal and Epithermal Neutron Ranges," International Conference on Nuclear Data for Science and Technology, Nice, France April-22-27, 2007.

[17] L.C. Leal et al. "R-Matrix Analysis of ^{235}U Neutron Transmission and Cross Section in the Energy 0 to 2.25 keV," Nucl. Sci. Eng. 131. 230 (February 1999).

[18] L. Erradi, A. Santamarina, and O. Litaize, "The Reactivity Temperature Coefficient Analysis in Light Water Moderated UO2 and UO2-PuO2 Lattices", Nucl. Sci. Eng. 144, 47-74 (2003).

[19] L.M. Bolinger, R.E. Cote, and G.E. Thomas, Bul. Am. Phys. Soc. 1, 187 (K5) 1956.

[20] C. Wagemans et al., Proc. Int. Conf. Nuclear Data for Science and Technology, Mito, Japan May 30-June 3, 1988.

[21] R. Gwin et al., Nucl. Sci. Eng. 45, 25 (1971).

[22] S.F. Mughabghab, "Atlas of Neutron Resonance Parameters and Thermal Cross Sections, Z=1-100," Elsevier 2006.

[23] SCALE: A Modular Code System for Performing Standardized Computer Analyses for Licensing Evaluations, NUREG/CR-0200, Rev. 7 (ORNL/NUREG/CSD-2/R7), Vols I, II, and III (May 2004).
[24] C. De Saint Jean et al., "*Uncertainty Evaluation of Nuclear Reaction Model Parameters Using Integral and Microscopic Measurements with the CONRAD Code"*, Journal of the Korean Physical Society, **59** (2011) 1276-1279.
[25] C. De Saint Jean et al., Nucl. Sci. Eng. 161, 363 (2009).
[26] B. Habert et al., Nucl. Sci. Eng. 166, 276 (2010).
[27] G. Noguere et al., Nucl. Sci. Eng. 172, 164 (2012).
[28] E. Lynn et al., Phys. Lett. 18, 31 (1965).
[29] E. Lynn, Rev. Mod. Phys. 52 (1980).
[30] G. LeCoq, Evaluation des données neutroniques pour le ^{239}Pu, PhD thesis, Orsay, France, 1967.
[31] H. Derrien, Etudes des sections efficaces de réaction des neutrons de résonance avec ^{239}Pu, PhD Thesis, Orsay, France, 1973.
[32] D. Shackleton, Etude des neutrons et des rayons gamma émis lors de la fission induites dans ^{235}U et ^{239}Pu par neutrons lents: mise en évidence de la réaction (n,γf), Orsay, France, 1974.
[33] J.E. Lynn, *Systematics for neutron reactions of the actinide nuclei,* AERE-R7468 (1974).
[34] O. Bouland et al., Phys. Rev. C 88, 054612 (2013).
[35] E. Fort et al., Nucl. Sci. Eng. 99, 375 (1988).
[36] R. Gwin et al., Nucl. Sci. Eng. 87,381 (1984).
[37] P. Leconte et al., submitted to PHYSOR 2014.
[38] K Shibata et al., JENDL-4.0: A New Library for Nuclear Science and Engineering, Journal of Nuclear Science and Technology 48(1), page 1-30 (2011).
[39] M.B. Chadwick et al., ENDF/B-VII.0: Next Generation Evaluated Nuclear Data Library for Nuclear Science and Technology, Nuclear Data Sheets 107, page 2931–3060 (2006).
[40] R. Capote et al., Summary report, consultants' meeting on Prompt Fission Neutron Spectra of major actinides, IAEA INDC(NDS)-0541 (2008).
[41] R. Letellier, C. Suteau, D. Fournier, J-M. Ruggieri, High Order Discrete Ordinate Transport in Hexagonal Geometry: a New Capability in ERANOS, Il Nuovo Cimento, 33C, (2010).